depascuales@ornl.gov

OAK RIDGE National Laboratory

June 12, 2025 | Fusion Energy Division

Integrated Plasma Modeling:

From the Power of the Sun to Powering Society on Earth

PRESENTED BY

Sebastian De Pascuale

PPPL SULI Introduction to Fusion Energy and Plasma Physics Summer School Course

U.S. DEPARTMENT OF ENERGY

ORNL IS MANAGED BY UT-BATTELLE LLC
FOR THE US DEPARTMENT OF ENERGY

About Me – From Astronomy to Space Physics

Grinnell College

University of Iowa

About Me – From Water Rocketry to Rowing on Water

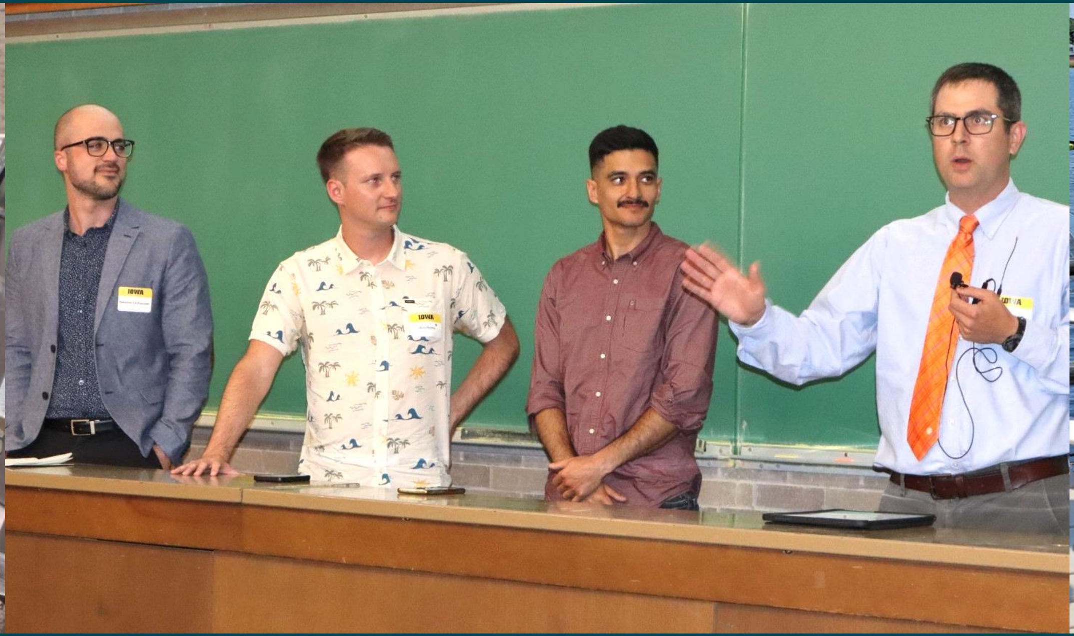

Knox County, Ohio

Knox County, Tennessee

My Trajectory into the Field of Fusion Energy Science

2011 – Los Angeles

Research Experiences for Undergraduates (REU)

2015 - Los Alamos

Space Weather Summer School (SWSS)

2018 - Oak Ridge

Post-Doctoral Research Associate (ORNL)

“Just as the system of the sun, planets and comets is put in motion by the forces of gravity, and its parts persist in their motions, so the smaller systems of bodies also seem to be set in motion by other forces and their particles to be variously moved in relation to each other and, especially, by the electric force”

Sir Isaac Newton, *Principia* (1687)

Exploring Dusty Horizons at University of California, Los Angeles

"Your reward will be the widening of the horizon as you climb"
- Cecilia Payne (figure from NASA's Mars Perseverance Rover)

*Undergraduate Mentor Dr. Michael Fitzgerald

How do you find exoplanets orbiting other stars?

- Observe light curves from the occlusion of a planetary body in front of a star, or observe the gravitational disturbance of smaller bodies to the surrounding circumstellar debris disk

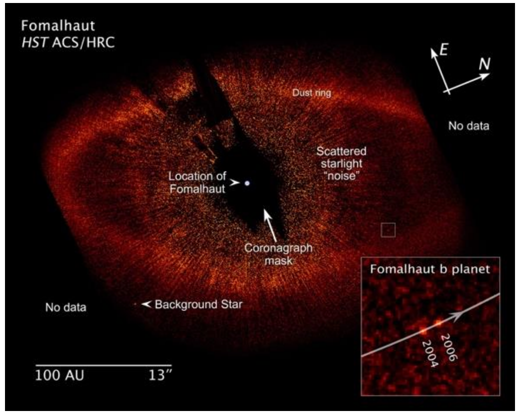

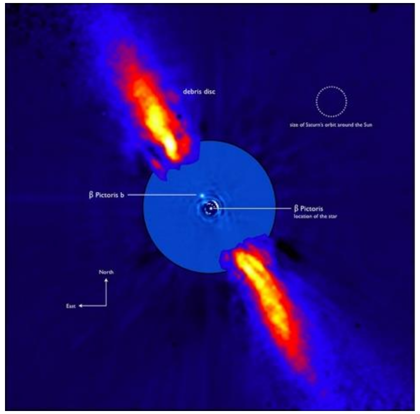

- Dust grain sized particles scatter light preferentially in the forward direction under Mie theory, causing the zodiacal light observed on Earth or the reddish haze observed on Mars

Oak Ridge National Laboratory

https://www.eso.org/public/images/eso0842b/
https://science.nasa.gov/wp-content/uploads/2023/04/fomalhaut_labeled-jpg.webp

https://usfusionenergy.org/opportunities

Illustration by Thumỹ Phan for U.S. Fusion Outreach

Cecilia Payne

What are stars made of? How do stars make their energy? We know the answers to these questions thanks to Dr. Cecilia Payne-Gaposchkin, who discovered that the stars, like our Sun, are mostly made of hydrogen and helium. This led to our understanding of fusion—the reaction that powers our sun and the stars. These elements are the “fuel” that powers fusion reactions inside the sun in a giant fusion engine. Together, we are working to build fusion engines here on Earth. Join the celebration and join the movement to bring the power of the stars to Earth.

Pursuing Complex Science at Los Alamos National Laboratory

How does space weather impact life on Earth?

- Geomagnetic storms are caused by the plasma connection of Earth’s magnetosphere with the enveloping solar heliosphere drawn out by coronal mass ejections and solar wind and flares

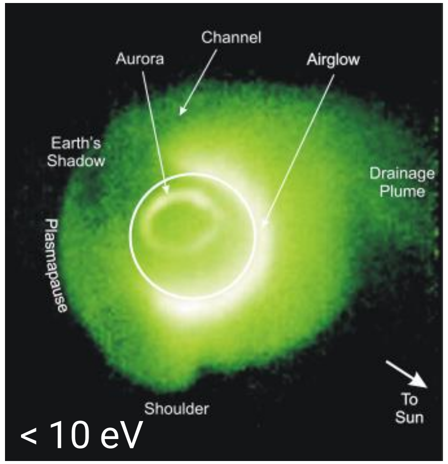

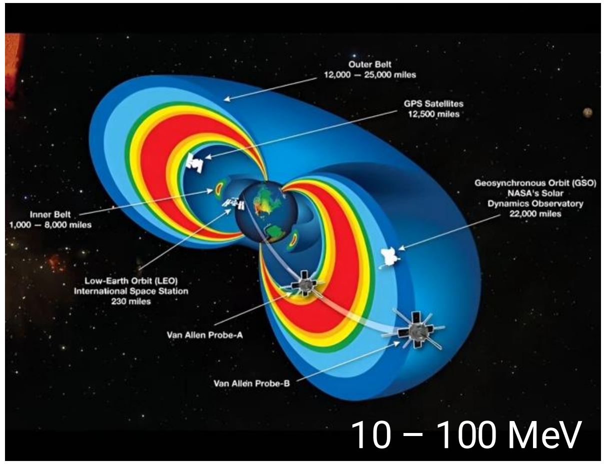

- Radiation belts trap energetic charged particles and can pose operational risks to commercial, national, and scientific satellites

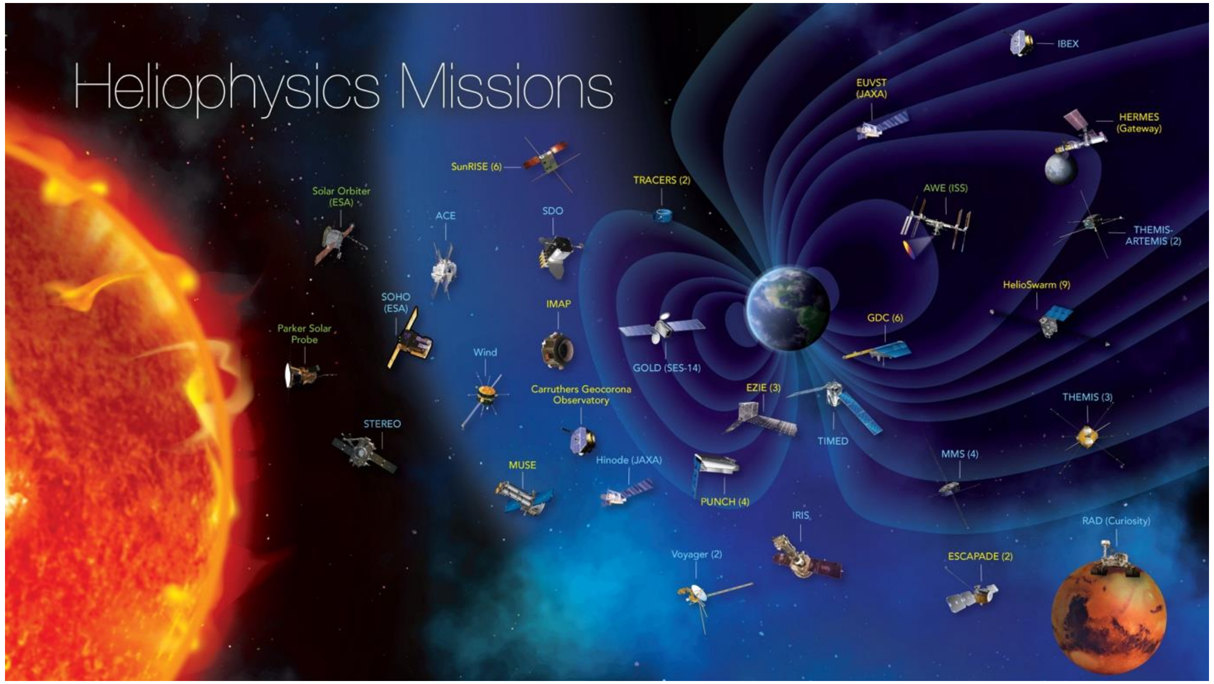

“I think the next [21st] century will be the century of complexity” -Stephen Hawking (figure from NASA GSFC Fleet ID:14718)

*Thesis Advisor Dr. Craig Kletzing and Vania Jordanova

- ❑ De Pascuale et al., JGR Space Phys., 2018 https://doi.org/10.1029/2018JA025776

https://phys.org/news/2024-08-scientists-phenomenon-impacting-earth-belts.html

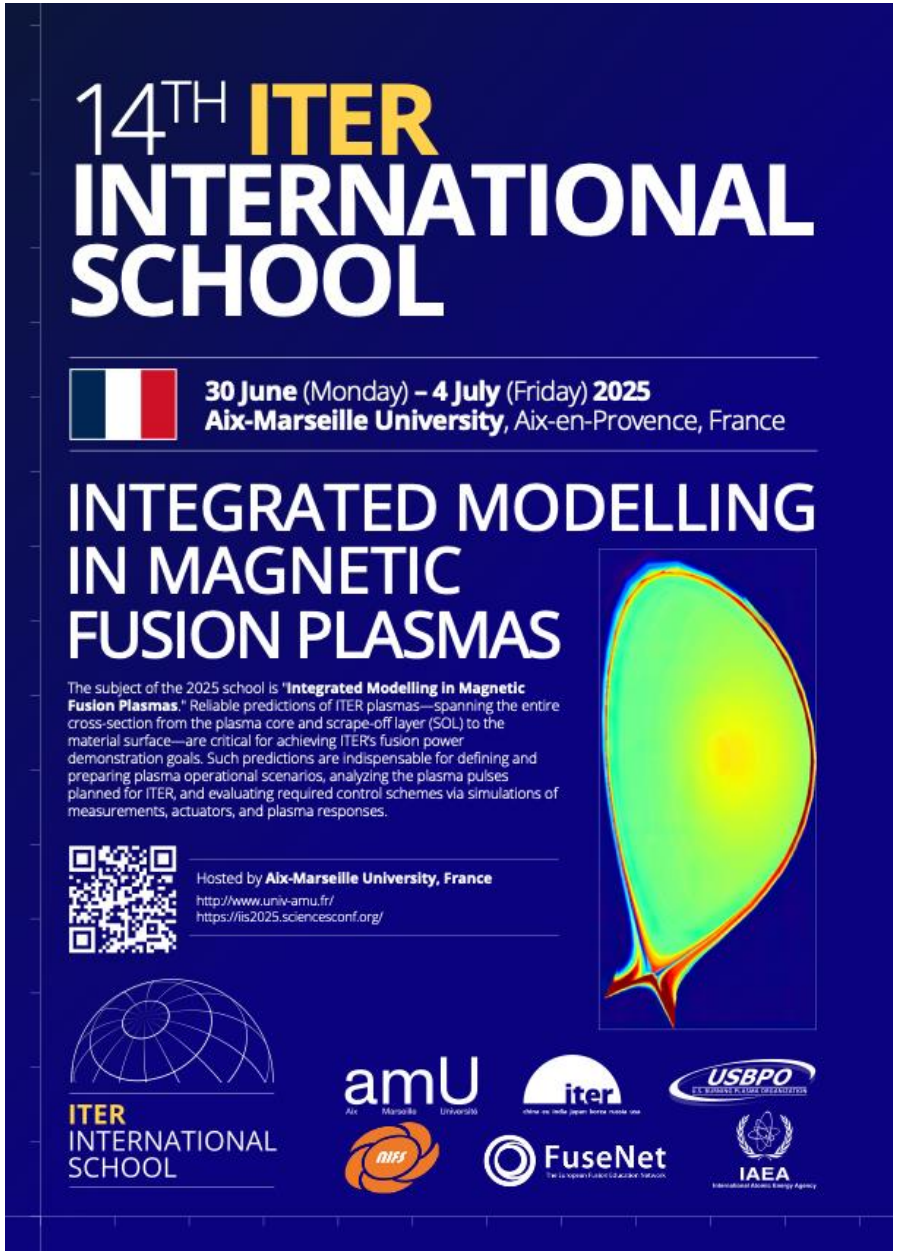

Summer Schools

ITER International School is organized nearly every year to offer early career scientists and engineers multi-disciplinary networking and instruction on the exciting field of nuclear fusion.

Each school is organized around a specific scientific theme and hosted by different countries around the world at institutions with access to tours of experimental research facilities.

Previous topics include:

- Diagnostics and Data Science
- Impacts of Energetic Particles
- Operation Scenarios and Control
- Technology of Power Flux Handling
- Transport and Pedestal Physics
- Disruptions and Magnetohydrodynamics
- High Performance Computing
- Plasma-Surface Interactions

https://iis2025.sciencesconf.org

Solving Big Problems at Oak Ridge National Laboratory

“We need people [at Oak Ridge] to solve big problems”
- Eugene Wigner (figure from ORNL Main Campus)

*Post-doc Advisor Dr. David Green

- ❑ De Pascuale et al., J. Comp. Phys., 2023 https://doi.org/10.1016/j.jcp.2023.112089

How can we accelerate progress towards fusion?

- High fidelity fusion simulations are computationally prohibitive without accounting for numerical limitations on the treatment of multiple scales

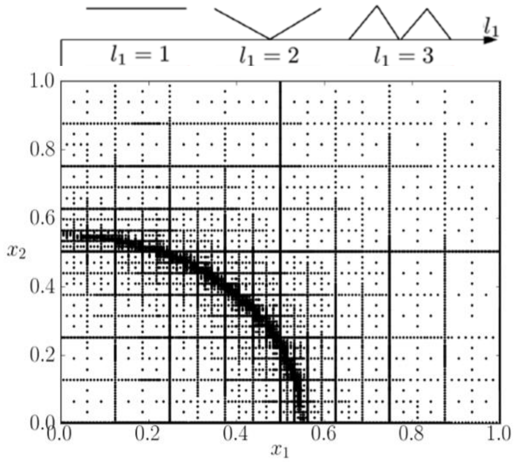

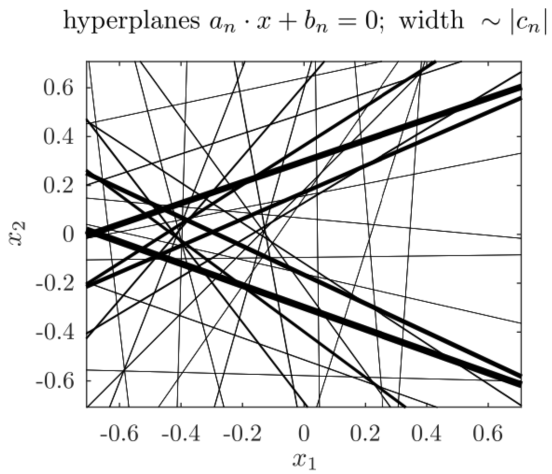

- Sparse discretization methods in space and time offer tractable approaches to reduce computational overhead and develop reduced models of governing physical systems

https://arxiv.org/pdf/1110.0010
https://arxiv.org/pdf/2410.02132

Research Internships

ORNL educational programs provide experiences complementing academic programs and enabling opportunities for additional learning, development, and training in a laboratory workplace setting.

Commitment to enriching scientific culture and the future workforce through **learning objectives** based, **mission aligned** experiences with world-class researchers, staff, facilities.

Over **20 program offerings** are available at any point in your developing career including elementary education, high school, undergraduate, community college, and graduate student participants.

See you at the traveling science fair or during a fall, spring, or summer internship!

https://education.ornl.gov

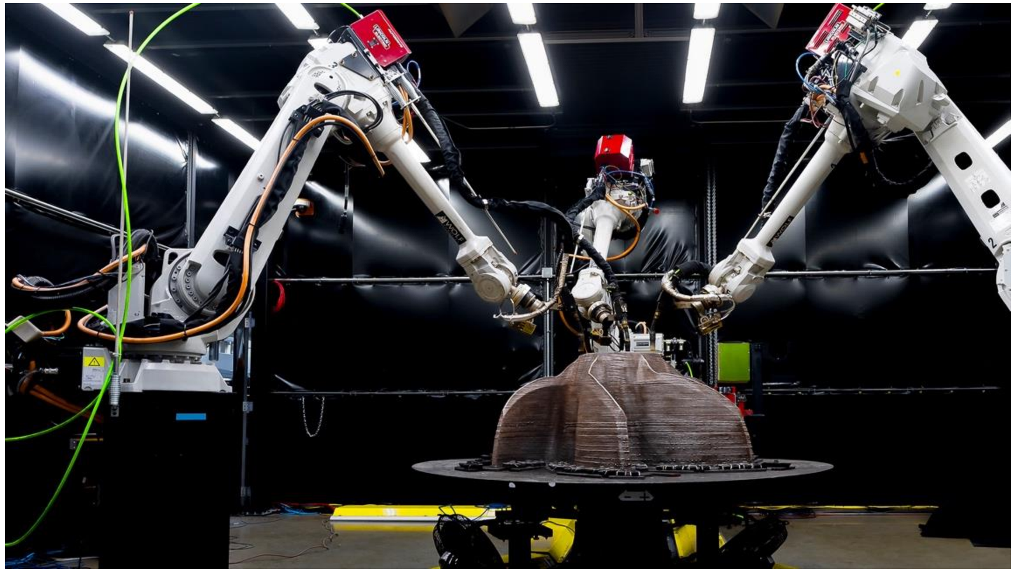

Three Takeway Themes

QUANTUM

Empowering scientists to pursue quantum innovation ›

FUSION

Fusion energy project among six ORNL Federal Laboratory Consortium wins ›

AI

Leading research to ensure secure, trustworthy, and energy efficient AI ›

Pearce et al., Proc. Natl. Acad. Sci, 2014; https://doi.org/10.1073pnas.1402202111

Cavagna et al., Nat. Comm., 2022; https://doi.org/10.1038/s41467-022-29883-4

First in Flight

"The period from 1885 to 1900 was one of unexampled activity in aeronautics, and for a time there was high hope that the age of flying was at hand…

But the public, discouraged by the failures and tragedies it had just witnessed, considered flight beyond the reach of humans, and classed its adherents with the inventors of perpetual motion…

Heavier-than-air flight had been ***around the corner*** for decades, with little to show for it…"

Controlled, powered flight

OAK RIDGE National Laboratory

*Wright Brothers (1903), Flyer I takes to the skies for just 12 seconds

Flying, with Contemporary Style

Fly-by-the-seat-of-your-pants

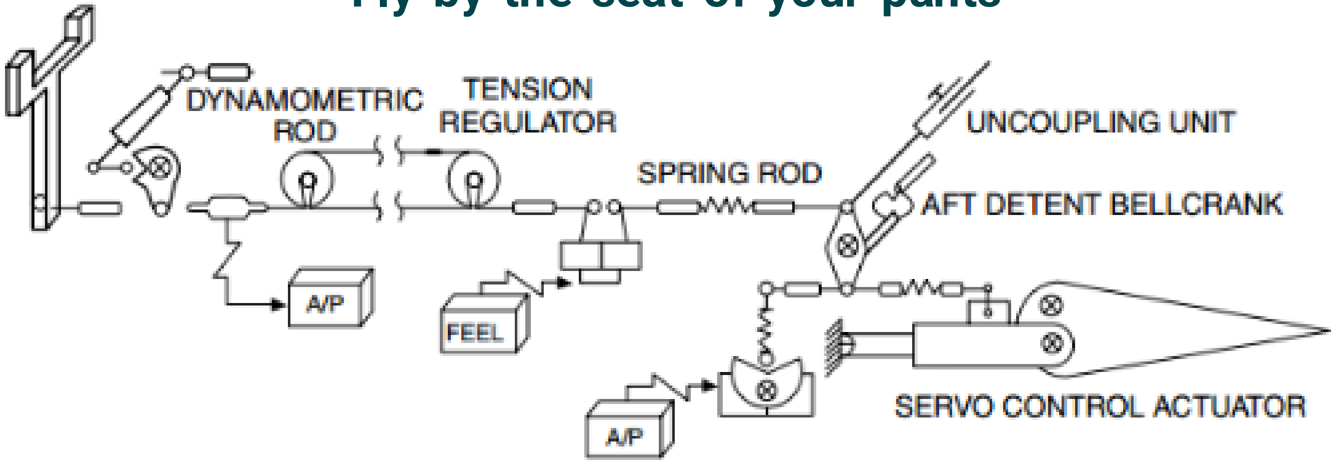

Fly-by-wire

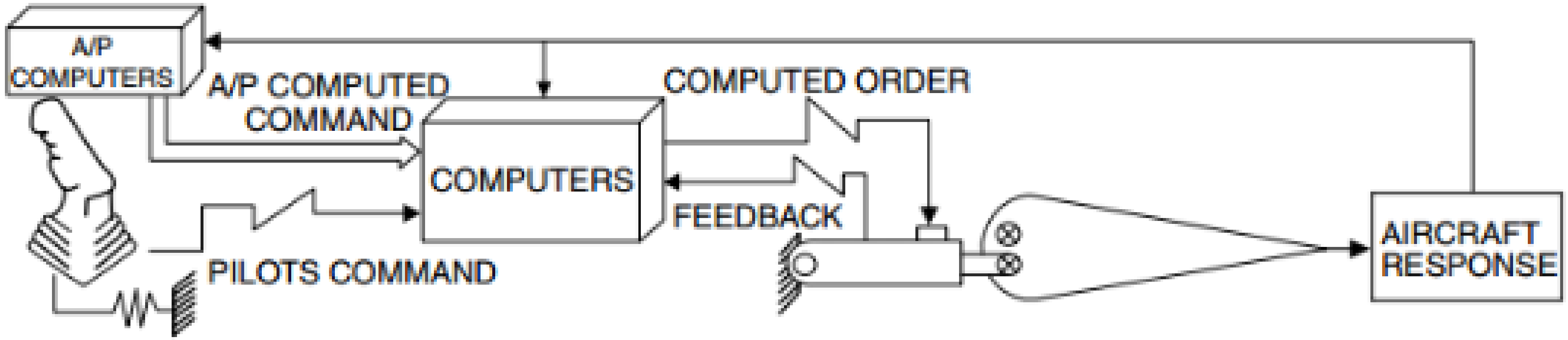

Flying, with Common Sense

Fly-by-autonomous-self-organization

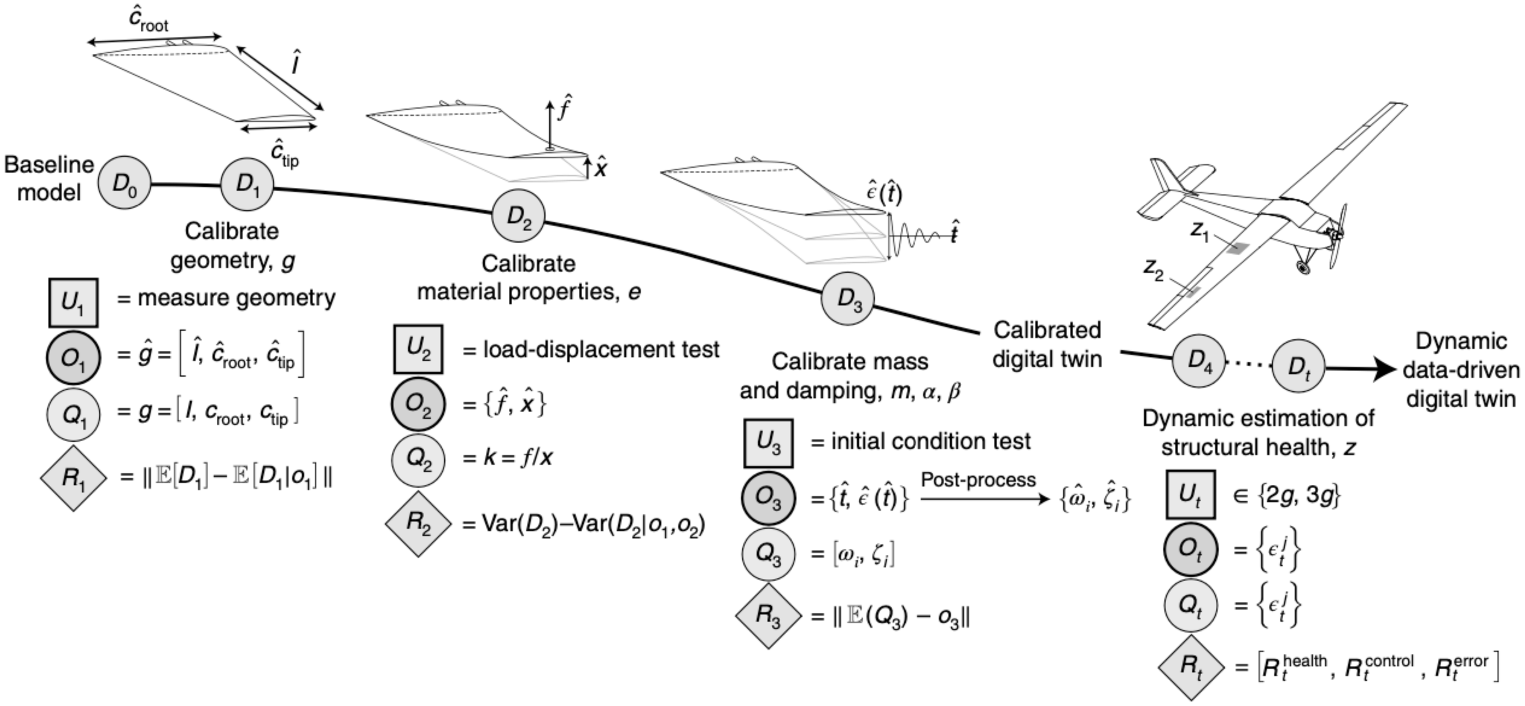

From Flight Simulator to Pulse Simulator

Designing a Digital Twin

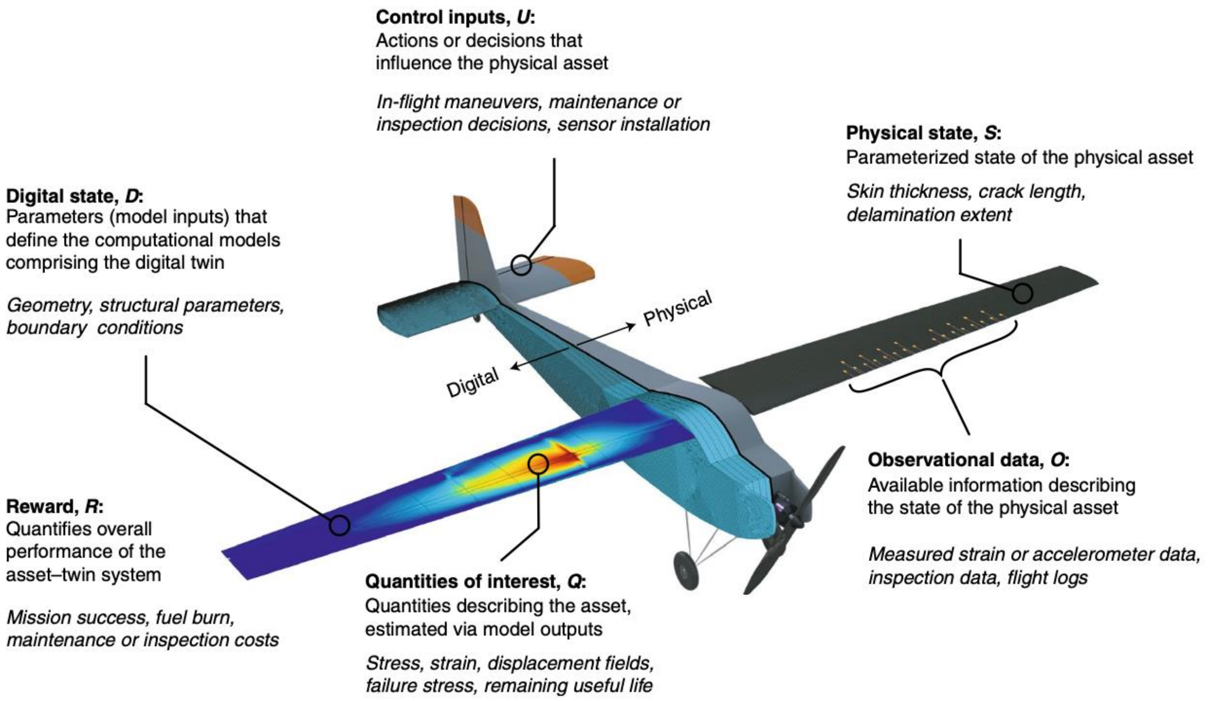

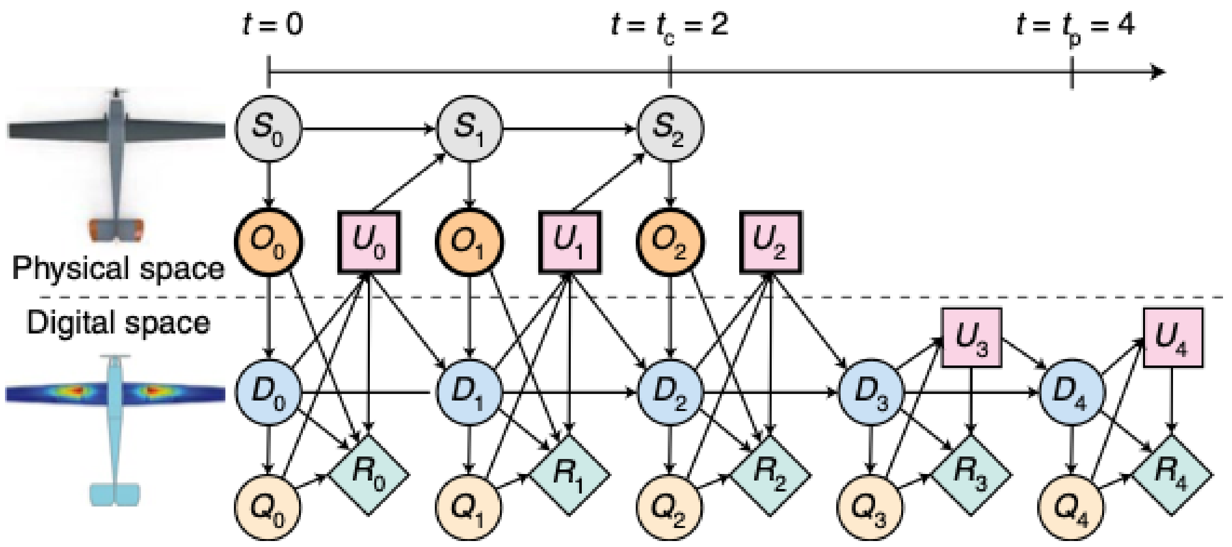

probabilistic graphical models with data assimilation

*Kapteyn et al., 2021, *Nature Comp. Sci*

First in Fusion – Putting Another Star on the Map

"Fusion is unquestionably one of the key technologies that will shape the coming millennium" following energy crisis of the 70s

In the 1980's Governor Alexander had a vision to create an Oak Ridge Corridor, and by 1995 an annual Science & Technology Summit was convened

During this time, fusion scaled back in enthusiasm, but reached new world records as well as substantial technological challenges

In 2010 "**Thirty years later**, tomorrow is here and –despite some delay– so is the bright promise" on ITER

Controlled, fusion power

*(1984), On the Man-Made Sun by T.A. Heppenheimer https://www.iter.org/node/20687/fusion-1980s-behind-scenes-look

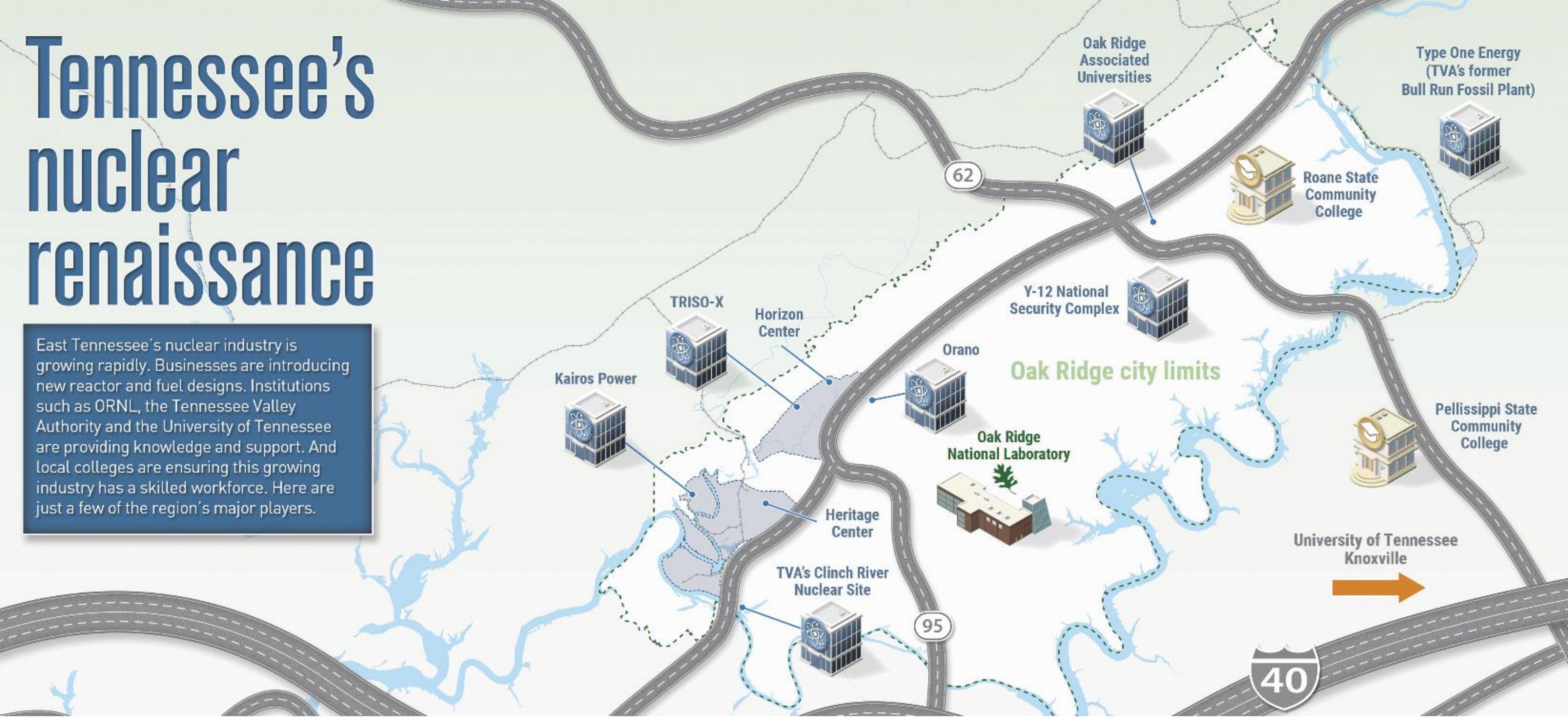

FUTURE FUSION ENERGY HUB

https://www.ornl.gov/nuclearishere

OAK RIDGE National Laboratory

Building Bridges for Public-Private Partnerships to Enable a Thriving Fusion Workforce and Industry Ecosystem

https://www.energy.gov/fusion-energy

https://typeoneenergy.com/potential-site-for-stellarator-fusion-prototype-machine-identified/

OAK RIDGE National Laboratory

Transport Processes are Inherently Multi-Scale and Ubiquitous Across the Entire Fusion Plasma System

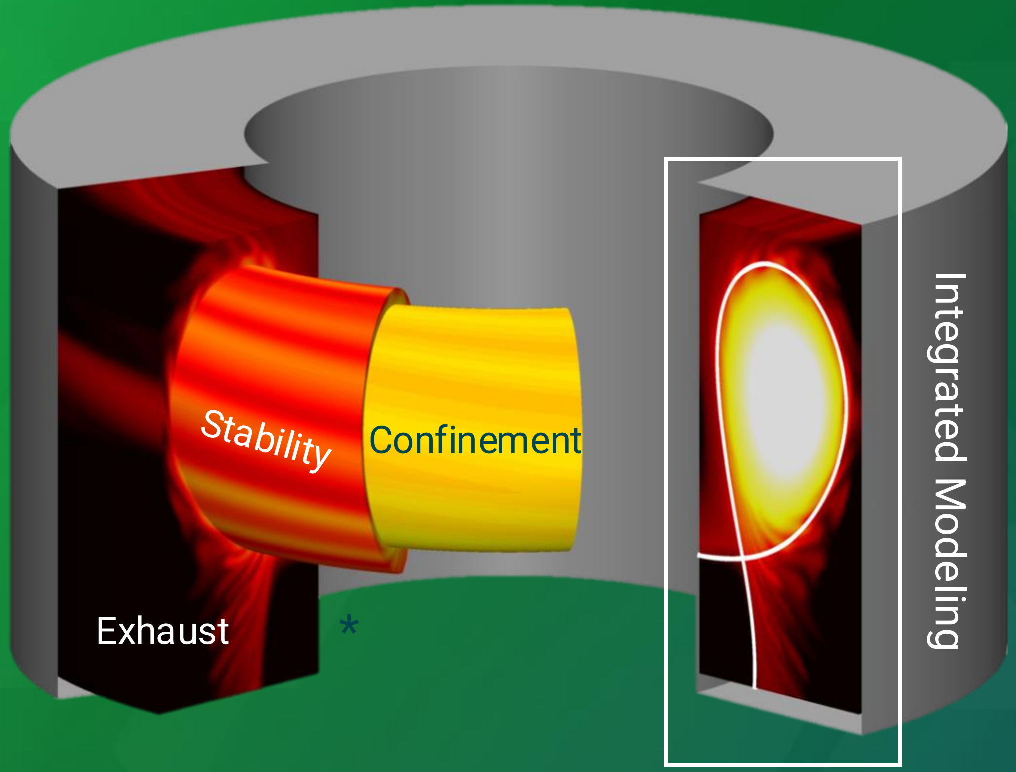

Core Confinement
- Maintain plasma performance under turbulence and other loss mechanisms

Edge Stability
- Manage high density and temperature against magnetohydrodynamic effects

Power & Particle Exhaust
- Mitigate plasma facing component exposures to damaging conditions

A hierarchy of simulation fidelities are required to achieve self-consistent tokamak plasma solutions

*Adapted from Giacomin et al., (2022), *JCP*, 463, 111294

Physics of Gyrokinetic Turbulent Transport in Tokamaks

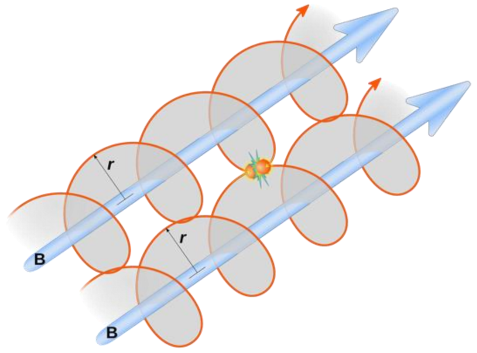

Classical Diffusion

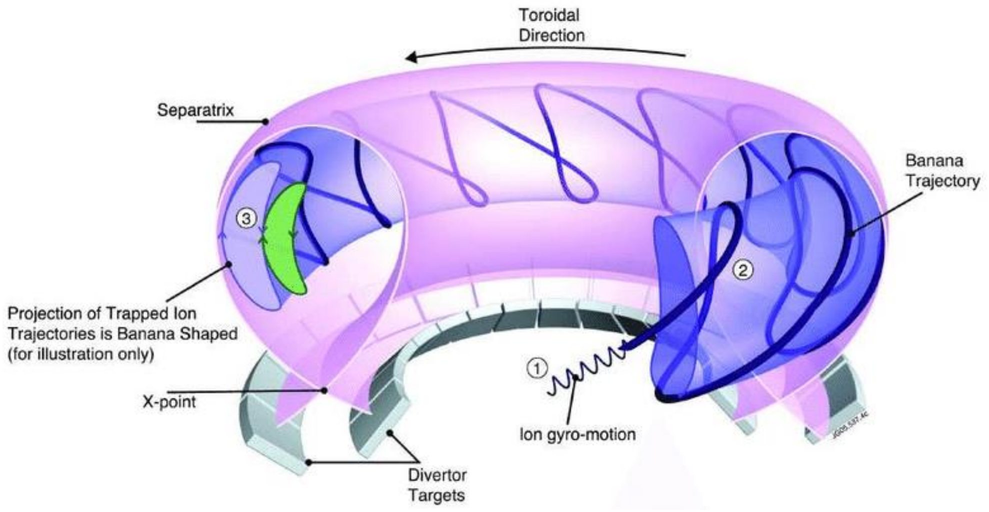

Neoclassical Transport

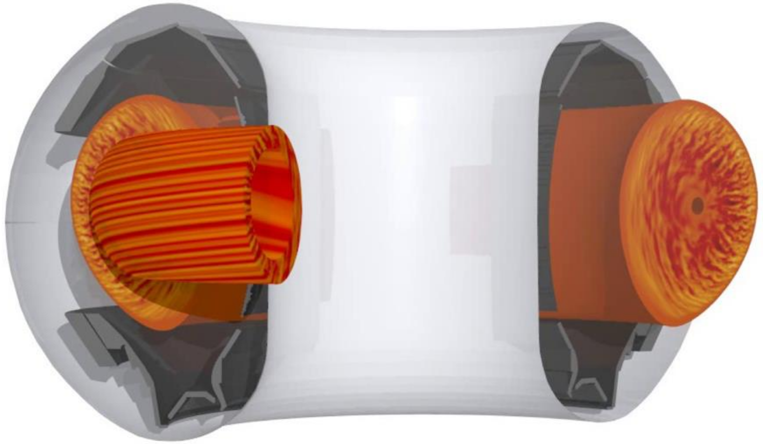

Turbulent Transport

Impact of Steep Gradients on Tokamak Edge Pedestal

Characteristic DIII-D Pedestal Scales

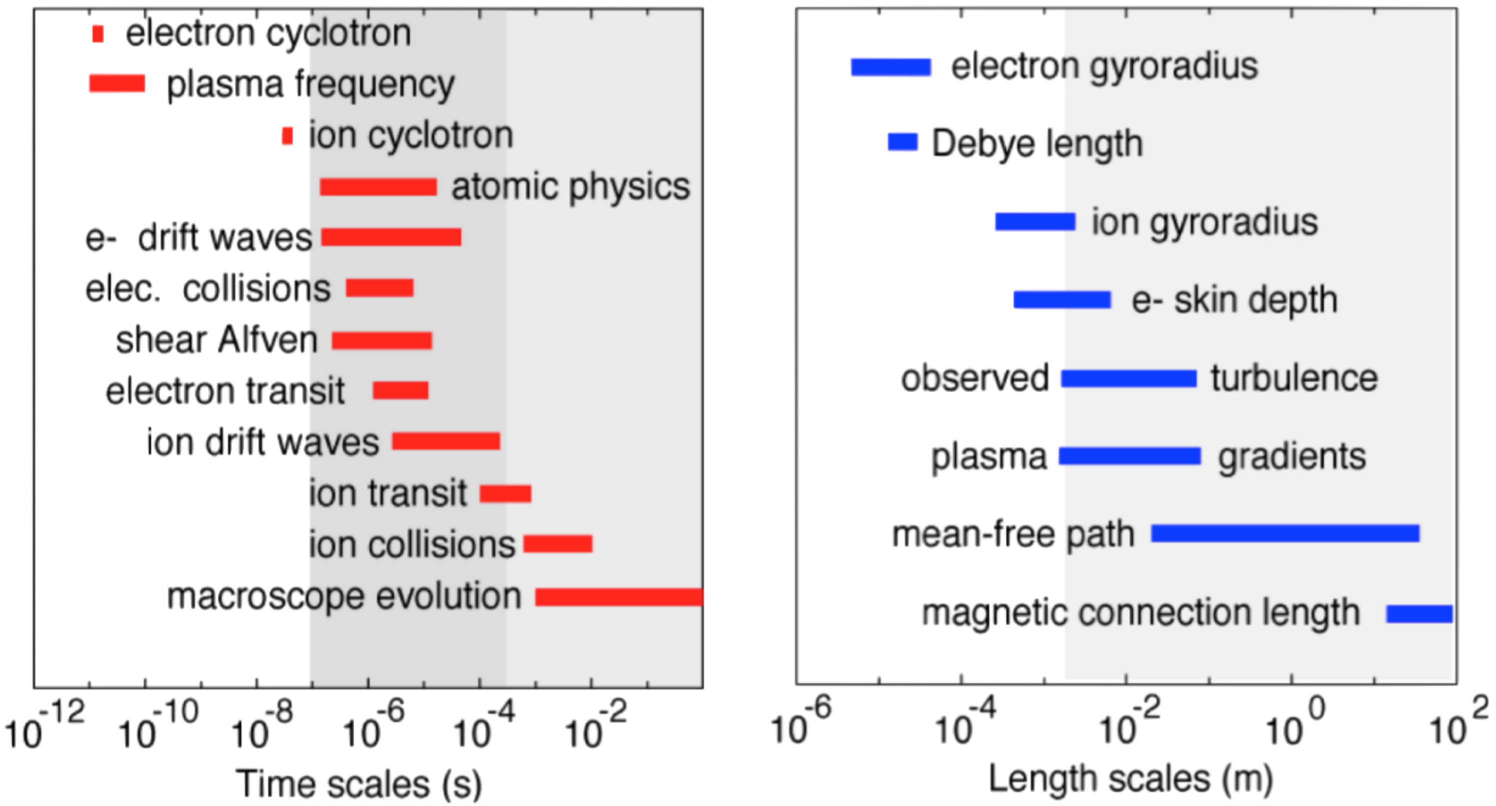

OAK RIDGE National Laboratory *Bonoli et al., 2015

Consequence of Tokamak Power Exhaust and Particle Control

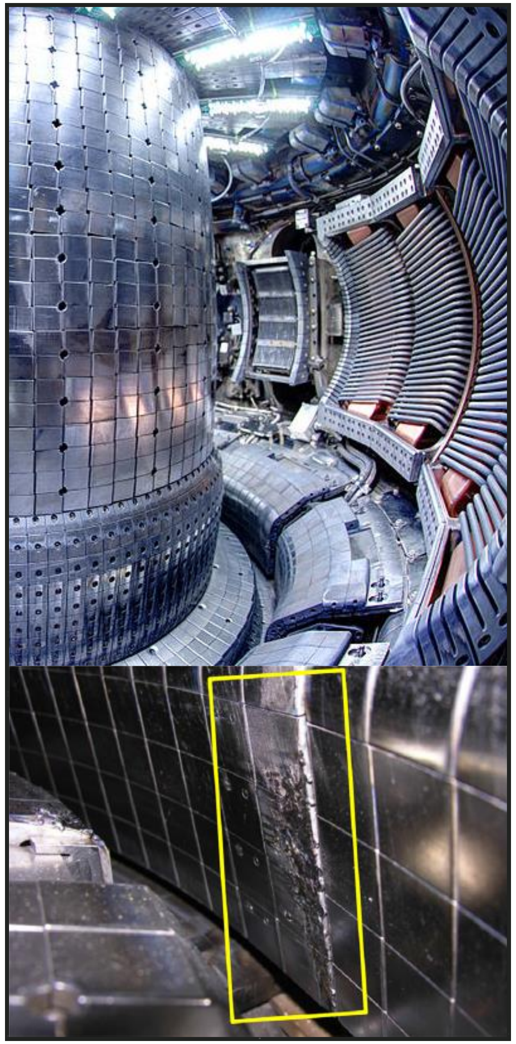

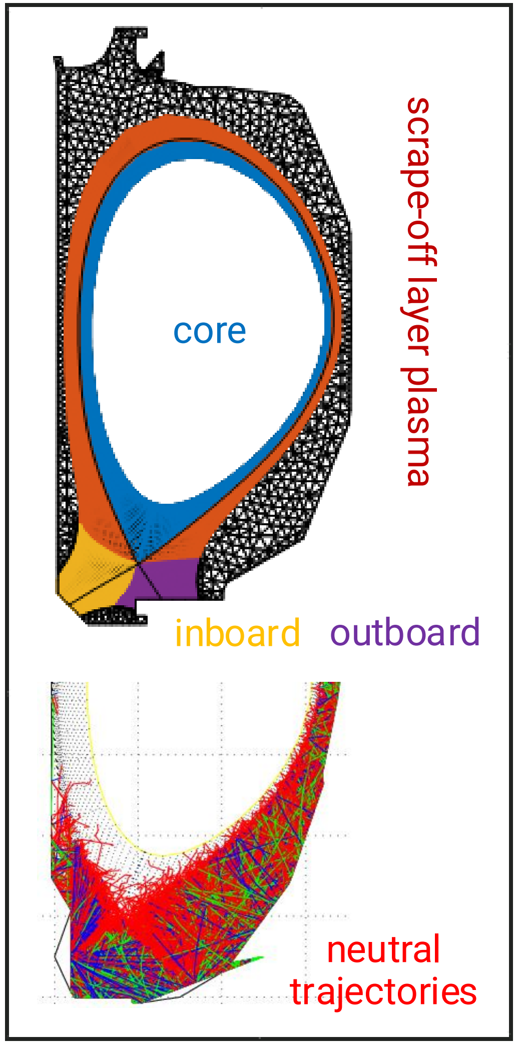

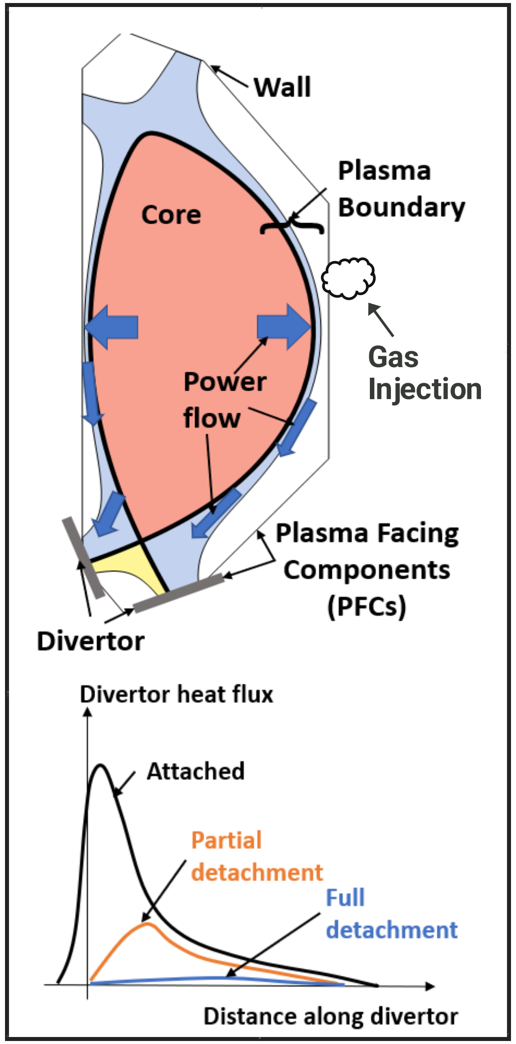

OAK RIDGE National Laboratory

[Arnas, et al., *Nuc. Mat. Energy* 2017 (Alcator C-Mod)

Integrated Modeling Captures Key Physics Regimes to Constrain Conditions on Behavior of Plasma Dynamics

τ_A — **Inherently Multiscale Regime** — τ_E

10^{-6} — 10^{-3} — 10^{0} sec

TGLF

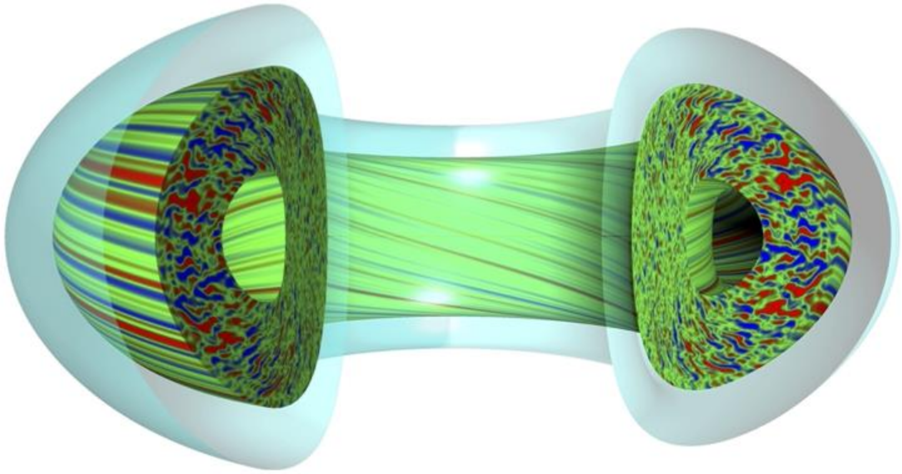

Trapped Gyro Landau Fluid

CPU-minutes

EPED

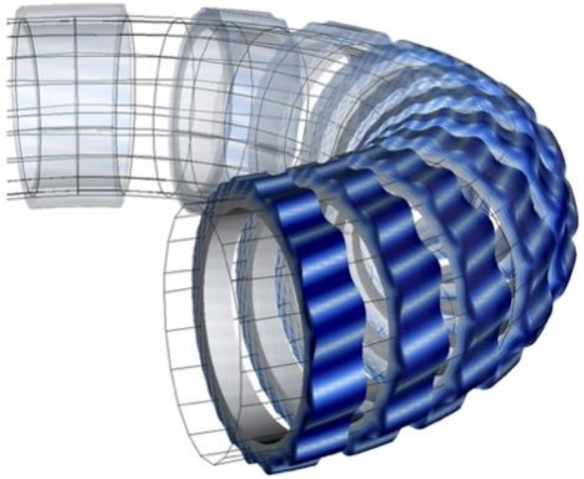

Edge Transport Barrier Pedestal

CPU-hours

SOLPS-ITER

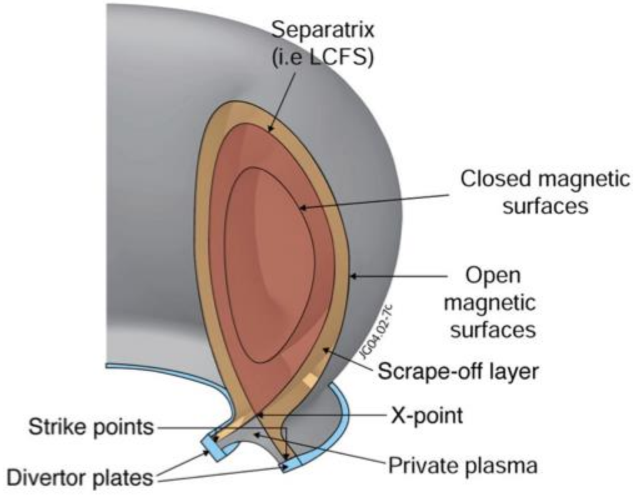

Scrape-off Layer Plasma Simulator

CPU-days

OAK RIDGE National Laboratory

Components of Experimental Control and Reactor Design

Tokamak Operations

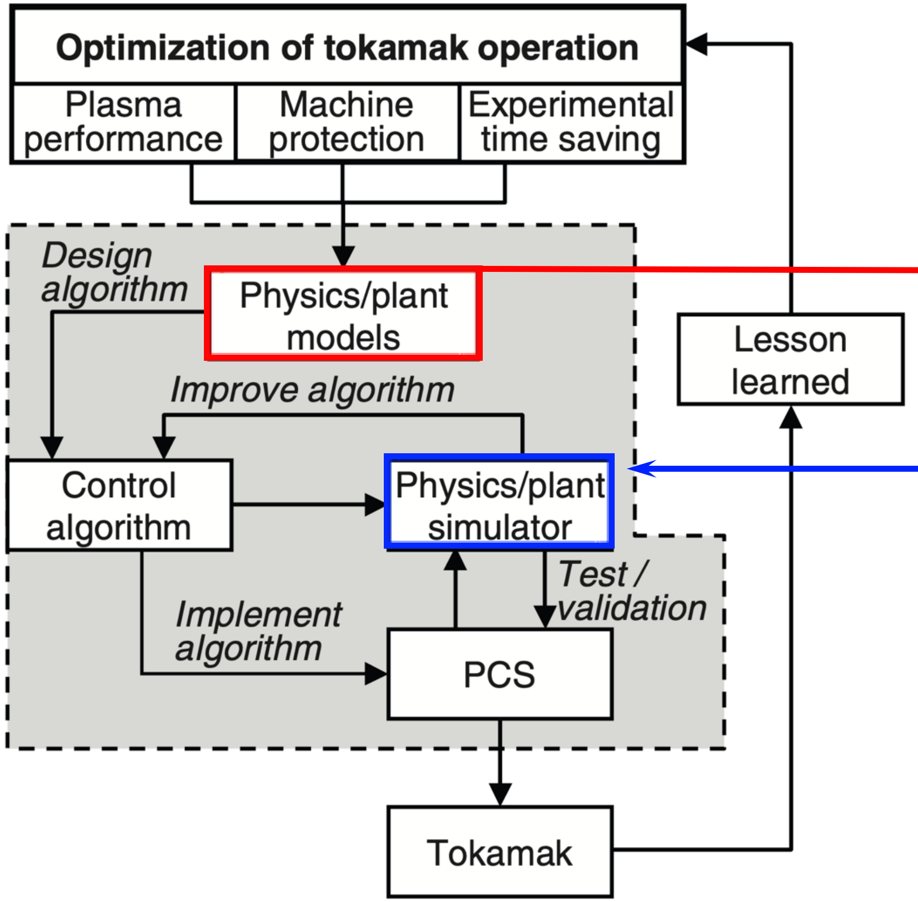

Tokamak Simulations

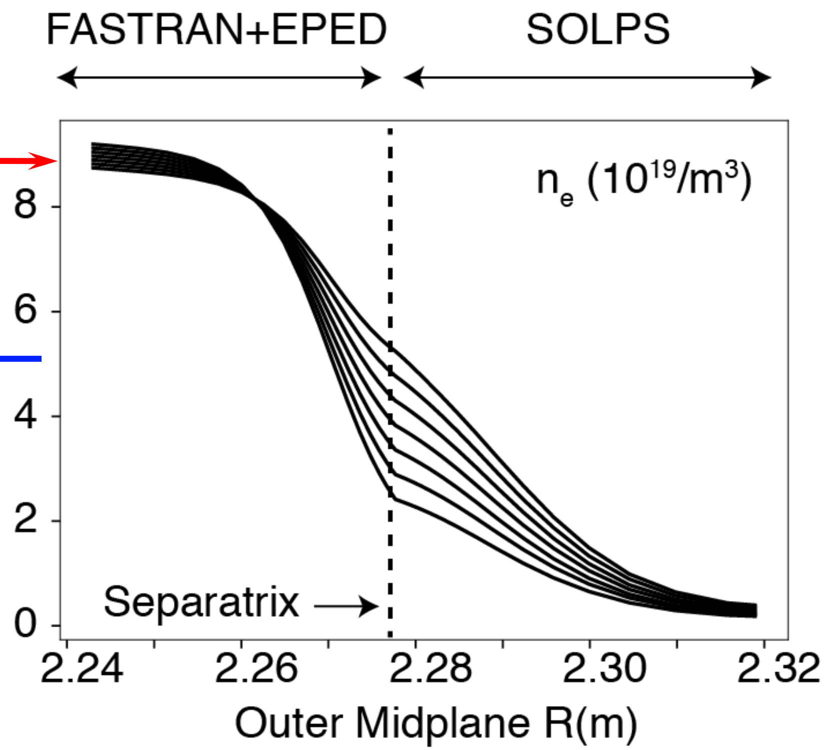

Components of Experimental Control and Reactor Design

Massively Parallel File-Based Model Coupling

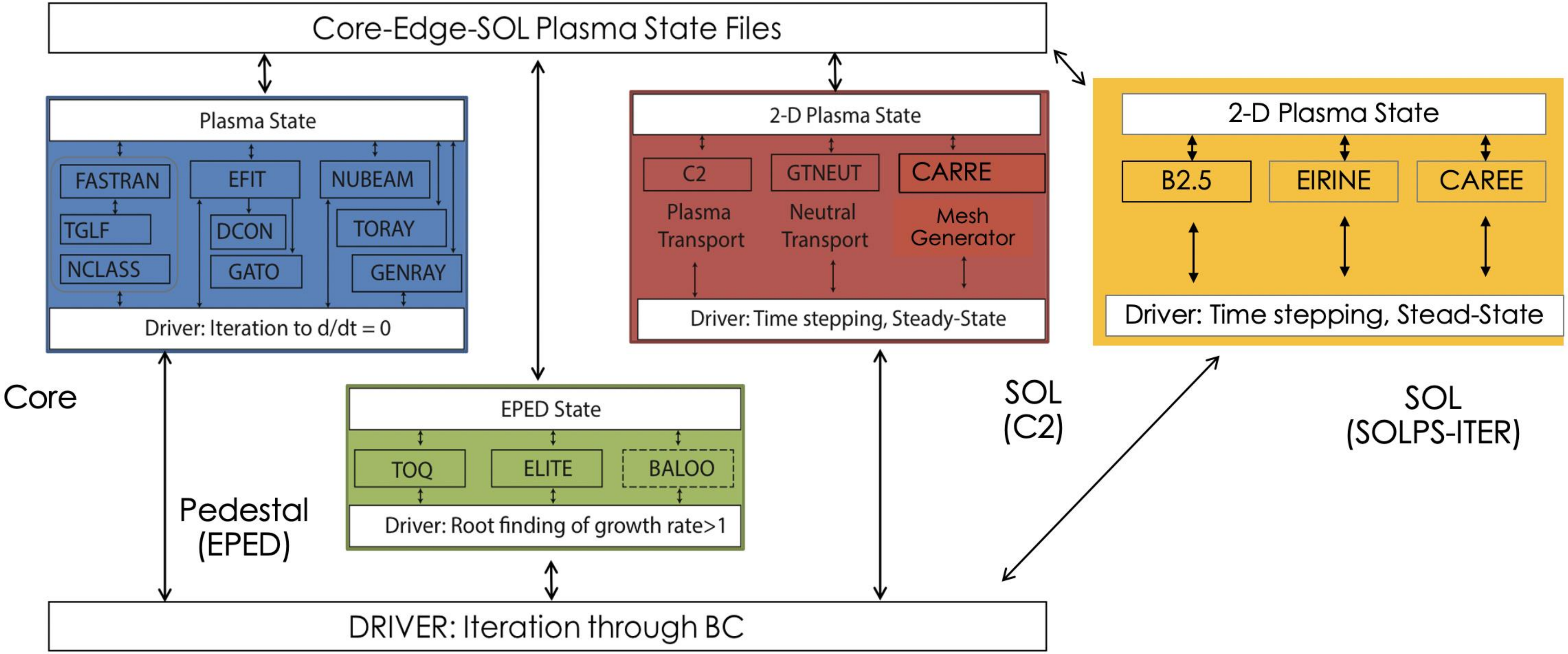

Components of Experimental Control and Reactor Design

Tokamak Shot Cycle

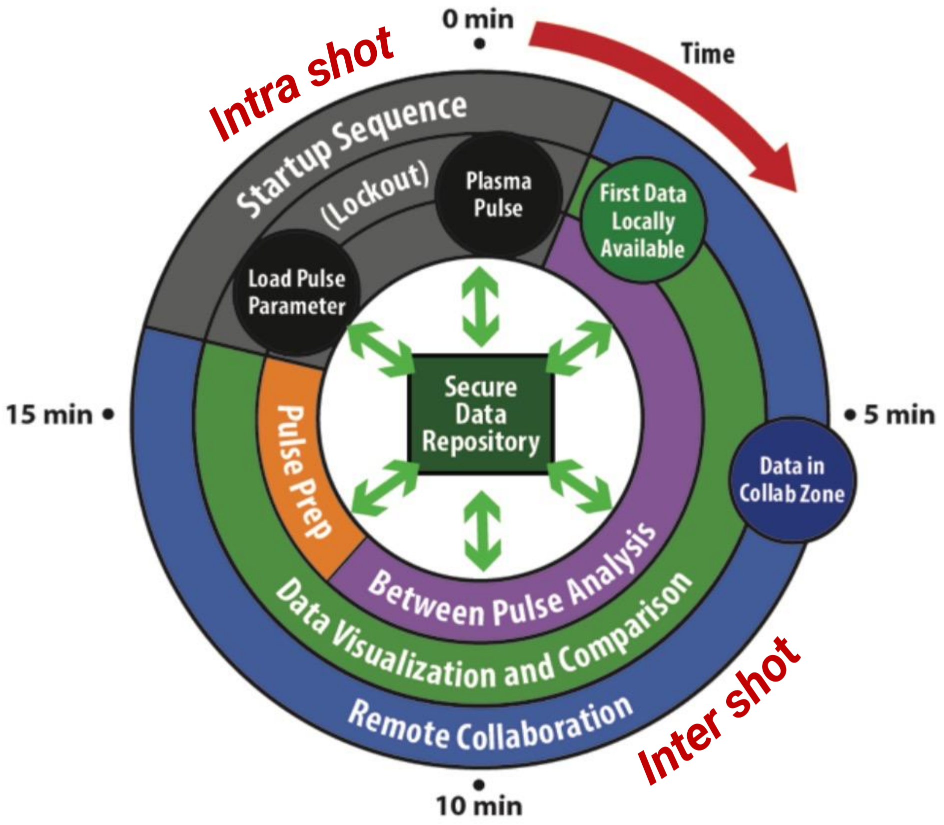

Integrated Plasma Simulator

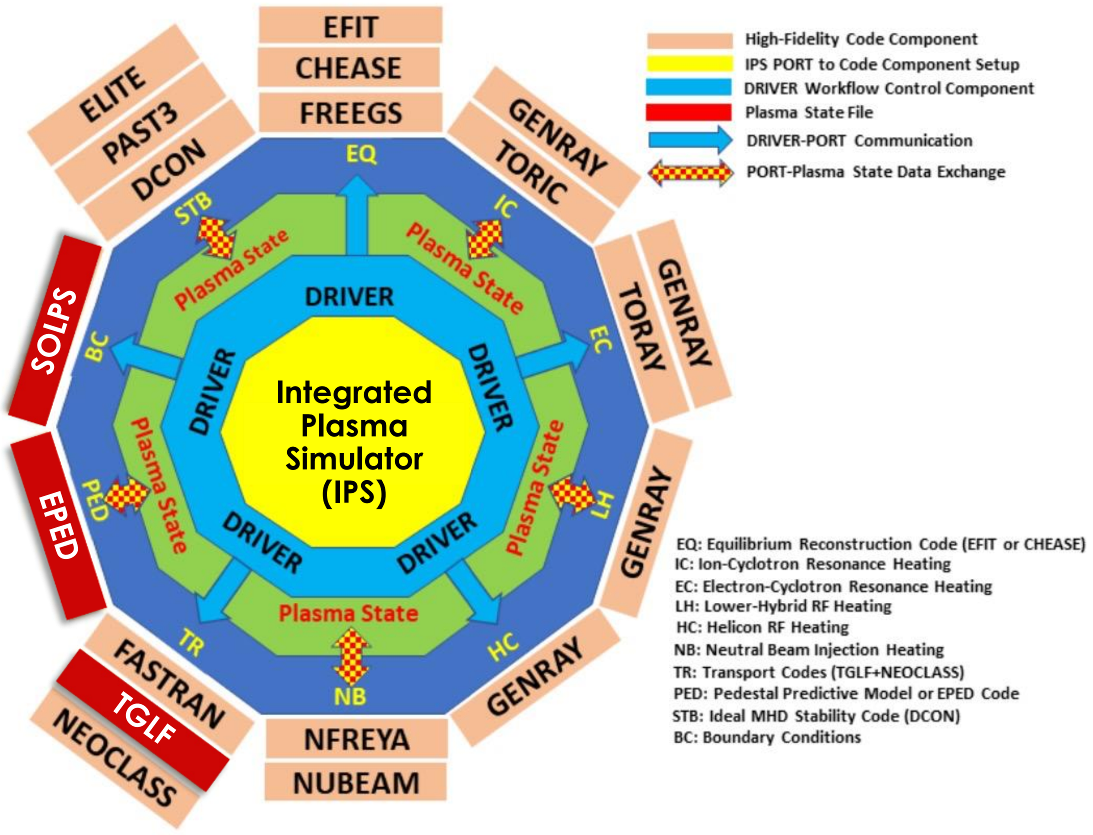

Reduced Models of Turbulent Transport Bridge Nonlinear Scales through Projected Linear Physics to Converged Saturation Level

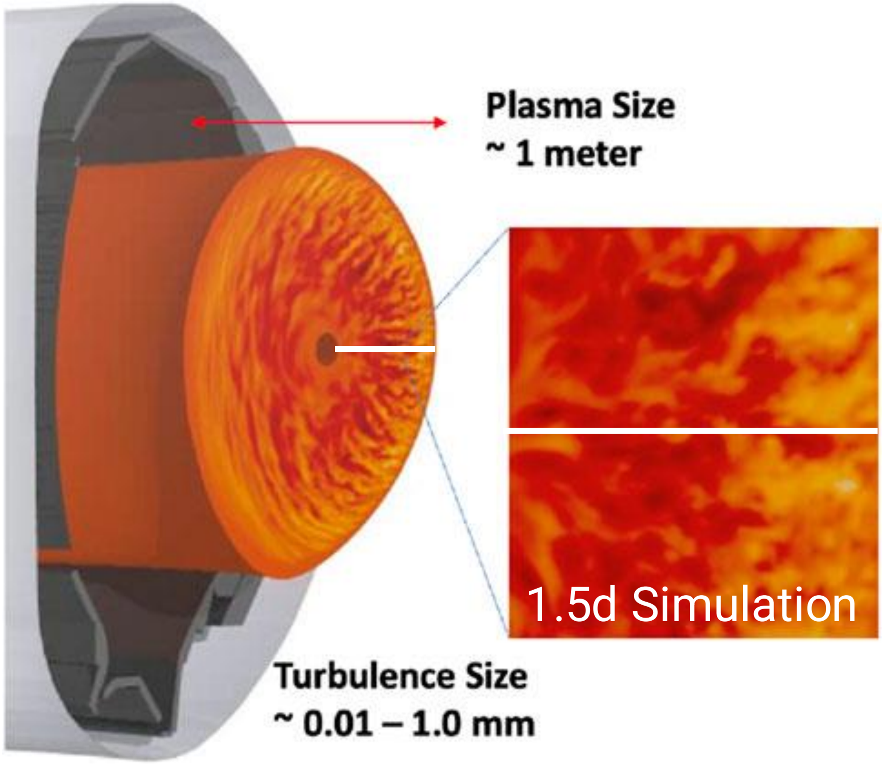

Converged Fluxes

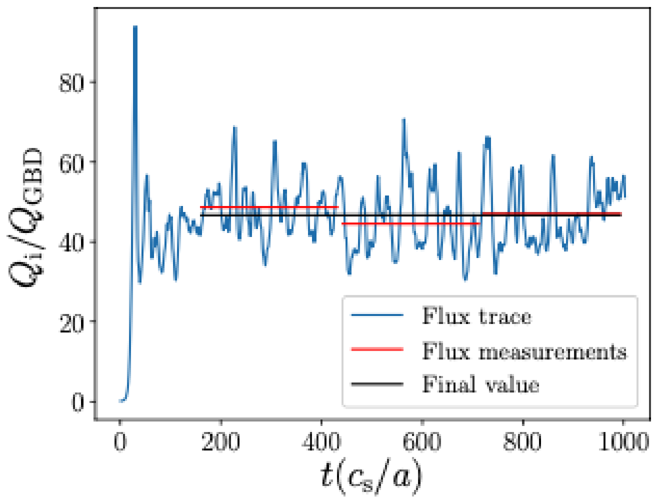

Saturation Rule

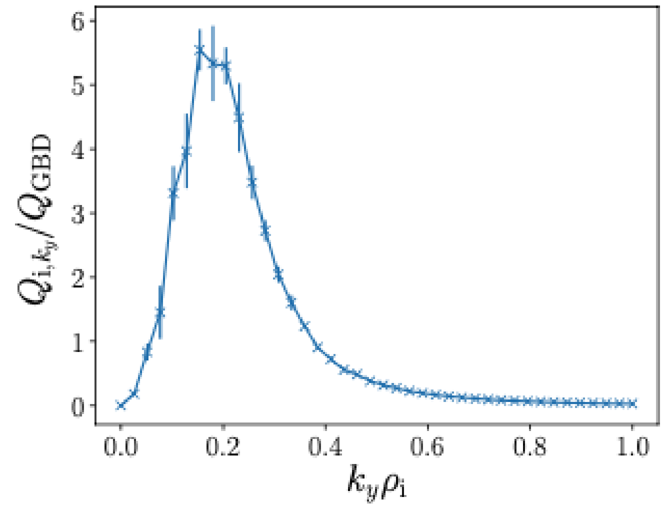

$$Q_s = 2\sum_{k_y>0} \Lambda_{s,k_y} W^{L}_{s,k_y} F_{s,k_y} \left[\frac{\left\langle \left|\delta\hat{\phi}_{k_y}\right|^2 \right\rangle_{x,\theta,t}}{\Delta k_y} \right] \Delta k_y$$

$$\frac{\left\langle \left|\delta\hat{\phi}_{k_y}\right|^2 \right\rangle_{x,\theta,t}}{\Delta k_y} = c_0 \sigma_{k_y}^{c_1}$$

OAK RIDGE National Laboratory

*GENE simulation and Dudding et al., Nucl. Fusion, 2022; https://doi.org/10.1088/1741-4326/ac7a4d

Saturation Rules Employ Multi-Fidelity Modeling to Capture Complex Interaction Between Physical Plasma Parameters

Linear Quantities

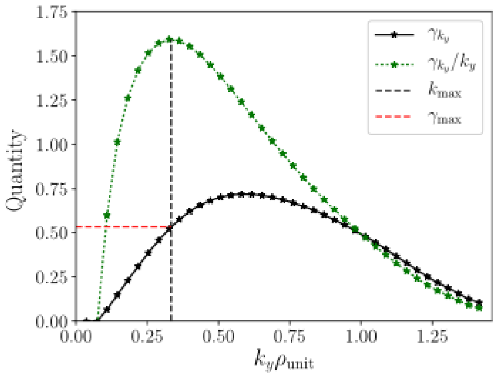

Saturated Potential

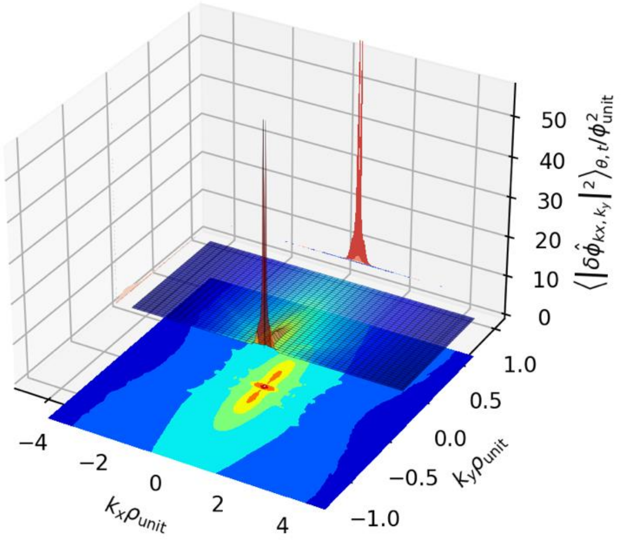

$$k_y, \gamma, \omega \longrightarrow \phi^2$$

Physical Parameter Space

Nucl. Fusion **62** (2022) 096005 H.G. Dudding *et al*

Table 1. Details of the 43 nonlinear CGYRO simulations that form the database. Note that the labels in the second column correspond with those in figure 13(*c*), used for discerning the cases displayed in figures 13(*a*) and (*b*), 17 and 18.

Varied parameter	Values (label)	Fixed	Isotopes simulated
— (GA-std)	— (a)	—	H, D, T
$a/L_{T_i} = a/L_{T_e}$	1.5 (b), 2.25 (c), 3.5 (d)	—	H, D, T
a/L_n	2.0 (e), 3.0 (f)	—	H, D, T
$\hat{s}$	0.25 (g), 0.5 (h), 1.5 (i)	$\hat{s}/w = 1/4$	D
$(a/c_s)\nu_{ee}$	0.01 (j)	—	H, D, T
$(a/c_s)\nu_{ee}$	1.0 (k)	—	D
T_i/T_e	0.5 (l), 1.5 (m)	—	D
q	1.5 (n), 2.5 (o)	—	D
κ	1.25 (p), 1.5 (q), 2.0 (r)	—	D
Δ	−0.125 (s), −0.25 (t), −0.5 (u)	—	D
r_0/R_0	1/4 (v), 1/12 (w)	—	D
$(a/c_s)\nu_{ee}$	0.01 (x)	$a/L_n = 3.0$	H, D, T
$(a/c_s)\nu_{ee}$	0.05 (y)	$a/L_n = 3.0$	H, T
$(a/c_s)\nu_{ee}$	1.0 (z)	$a/L_n = 3.0$	D

Oak Ridge National Laboratory *Preeti Sar (FED)

Global Quasilinear Transport is Governed by High-Dimensional Parameter Space Prohibiting Comprehensive Model Sampling

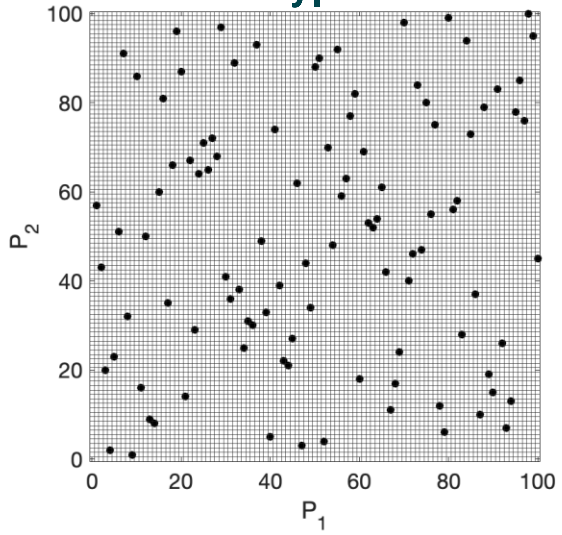

$s - \alpha$

https://zenodo.org/records/3274234

QuaLiKiz 4D, Citrin et al., (2015), *NF*, 55, 092001
QuaLiKiz 6D, Citrin et al., (2023), *PoP*, 30, 062501
QuaLiKiz 10D, van de Plassche (2020), *PoP*, 27, 022310

- Express curse of dimensionality when increasing degrees of freedom

QuaLiKiz 15D, Ho et al., (2020), *PoP*, 28, 032305

Dataset	Points	Time (CPU h)
10D	$\sim 3 \times 10^8$	$\sim 10^6$
Projected 15D	$\gtrsim 7.2 \times 10^{10}$	$\gtrsim 3 \times 10^8$
Actual 15D	3.38×10^7	3.5×10^5

- Supplement training data through experimental observations

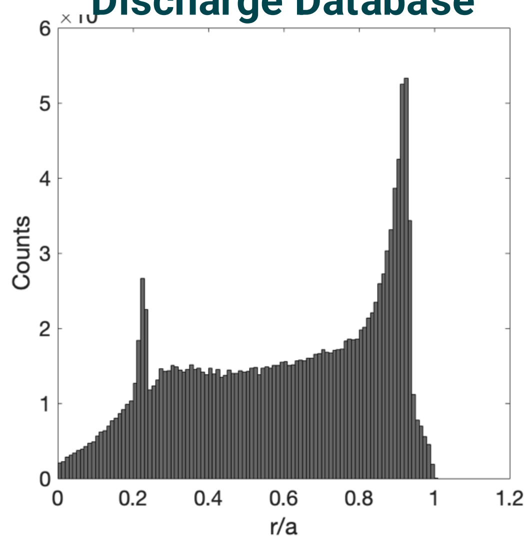

$R(r, \theta | \kappa, \delta)\ Z(r, \theta | \kappa, \delta)$

https://zenodo.org/records/3274234

TGLF 21D, Menenghini et al., (2014), *PoP*, 21, 060702
TGLF 23D, Menenghini et al., (2017), *NF*, 57, 086034

Fully 5D **gyrokinetic simulations** take on the order of **10^4 hours** of wall clock time per radial point

Oak Ridge National Laboratory

Local Dimensionless Plasma Parameters Have Associated Correlations and Accessibility in Present and Future Device

Principal Components

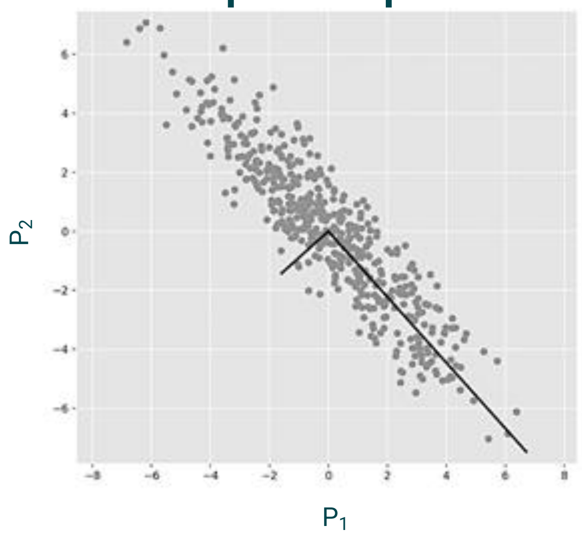

$$M = \sum_{i=1}^{n} \sigma_i \boldsymbol{u}_j \boldsymbol{v}_j^*$$

$$\|\boldsymbol{M} - \boldsymbol{M_r}\|_F = \sqrt{\sigma_{r+1}^2 + \cdots + \sigma_N^2}$$

- Gyrokinetic validation data is several orders of magnitude more expensive

TGLF-GKNN, Neiser et al., (2024) *TTF Conference*

Saturation Rule	Validation	Machines
SAT0,1,2,3	CGYRO	DIII-D/MAST-U

- Supplement quasilinear model performance through residual

K-Means Clustering

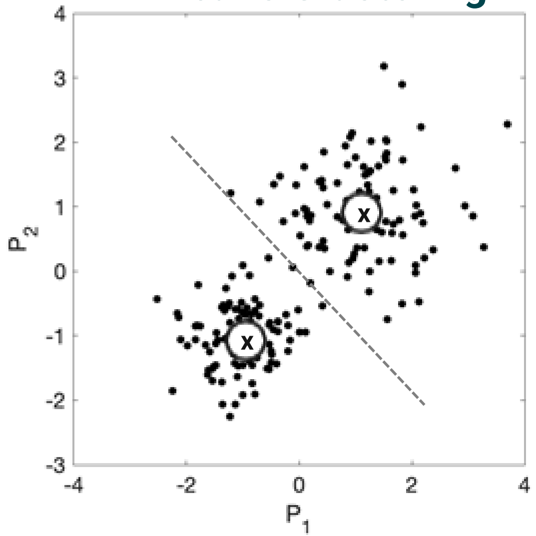

$$\mu_i = \frac{1}{|S_i|} \sum_{y \in S_i} y$$

$$\sum_{i=1}^{k} \sum_{x \in S_i} \|x - \mu_i\|^2 = \sum_{i=1}^{k} |S_i| \mathrm{Var}\, S_i$$

Quasilinear models, such as the **Trapped Gyro Landau Fluid (TGLF)**, reduce this cost down to **10^0 seconds**

Matrix Factorization Cannot Fully Capture Nonlinear Relationships in Feature Space of Simulation Domain

Variable	Definition
r/a	Normalized minor radius
R/a	Normalized major radius
κ	Elongation
$r\frac{\partial\kappa}{\partial r}$	Elongation shear
δ	Triangularity
$\frac{\partial R}{\partial r}$	Shafranov shift
q	Safety factor
$\frac{q^2a^2}{r^2}\frac{\partial q}{\partial r}$	Safety factor shear
β_e	Kinetic to magnetic pressure ratio
ν_{ie}/ac_s	Collision frequency
T_i/T_e	Ion to electron temperature ratio
n_D/n_e	Deuterium to electron density ratio
n_C/n_e	Carbon to electron density ratio
Z_{eff}	Effective ion charge
a/L_{Te}	Electron temperature scale length
a/L_{Ti}	Ion temperature scale length
a/L_{ne}	Electron density scale length
a/L_{nD}	Deuterium density scale length
a/L_{nC}	Carbon density scale length
$\frac{qa^2}{rB_{unit}^2}\frac{\partial p}{\partial r}$	Total pressure gradient
$\mathrm{sign}(I_p)R\omega_{tor}\frac{a}{c_s}$	Parallel velocity
$-\mathrm{sign}(I_p)R\frac{\partial\omega_{tor}}{\partial r}\frac{a}{c_s}$	Parallel velocity gradient
$-\mathrm{sign}(I_p)\frac{r}{q}\frac{\partial\frac{V_{E\times B}}{R}}{\partial r}\frac{a}{c_s}$	$E\times B$ velocity shear

Menenghini et al., (2017) *NF*, 57, 086034

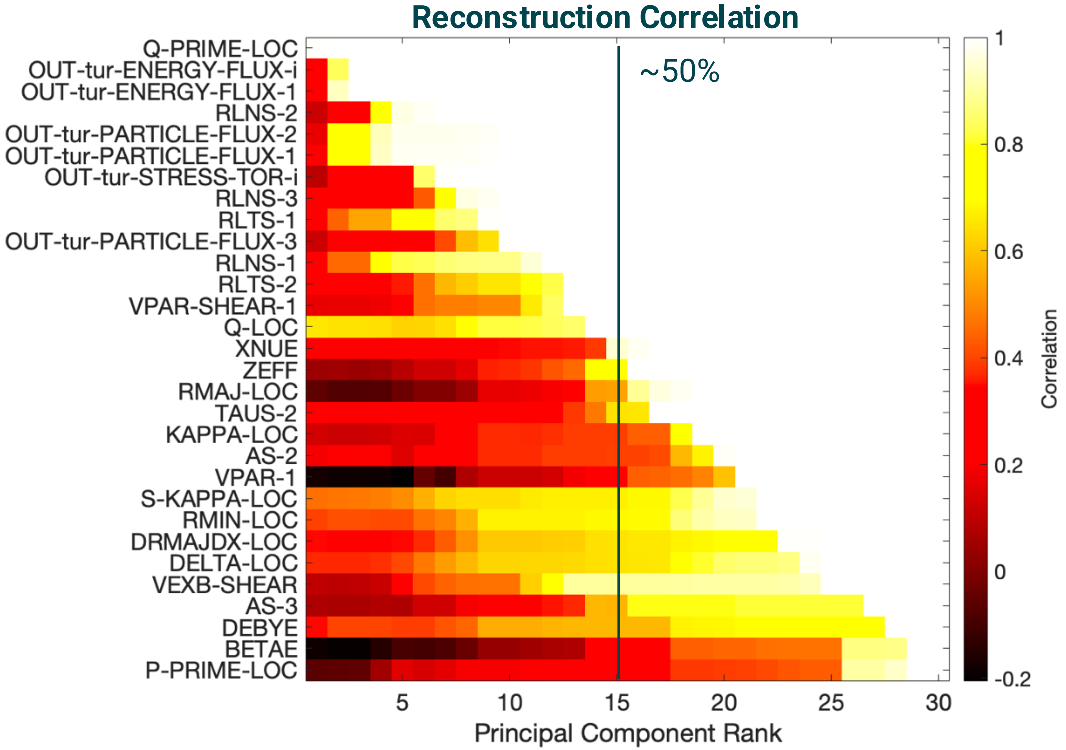

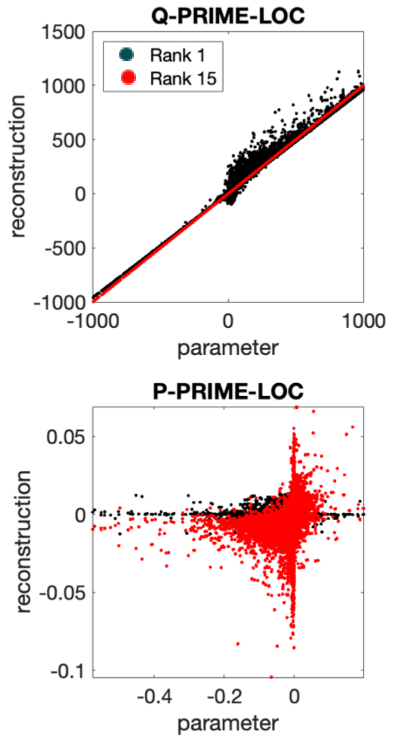

Surveyed database of DIII-D TGLF simulations spans **24D inputs** and **6D outputs** over range of experimental conditions and nearly 1.6 million points

Vector Quantization Groups Nearest Neighbor Simulations Separating Out Over-Sampled Parameter Regions in Domain

Input by Input

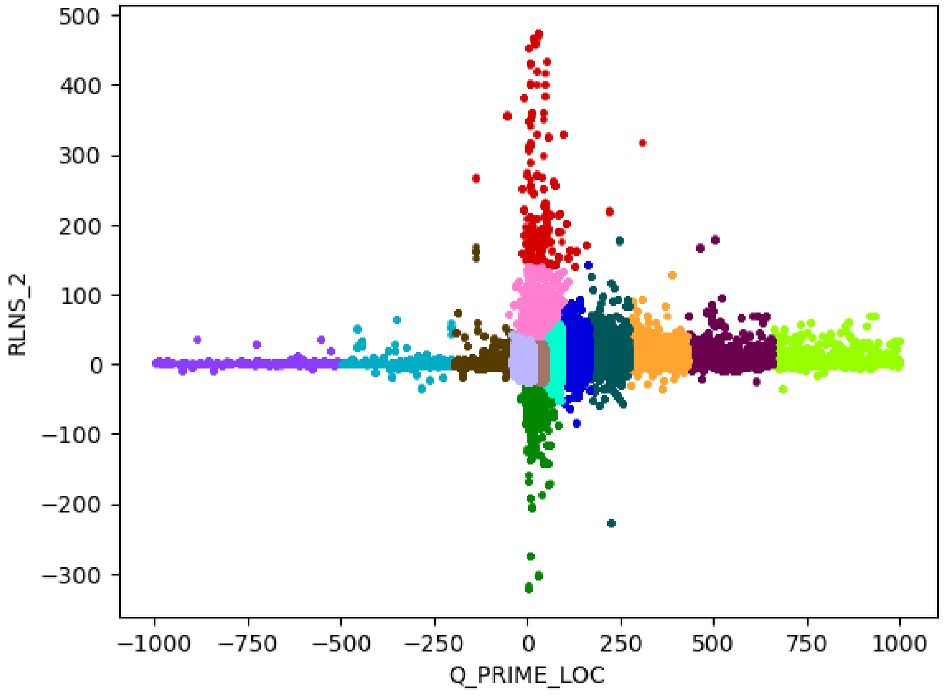

20% Compression

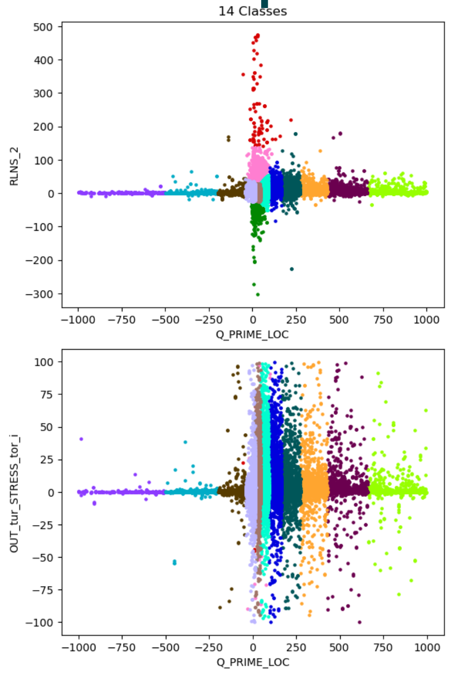

Input by Output

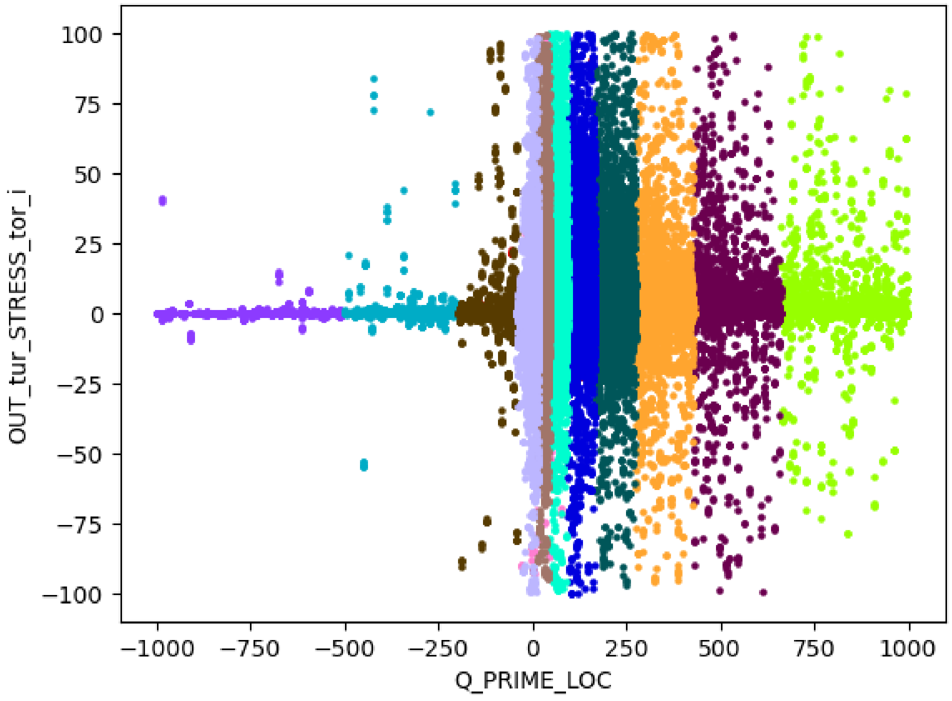

Dataset can be compressed by nearly an **order of magnitude** when clustered in the input space alone, reducing the number of simulations required for machine learning

Accelerated Predictions of Quasilinear Transport Simulations in Many Degrees of Freedom Are Enabled by Machine Learning

XGBoost: gradient boosted split level branching tree

- memory efficient
- fast to train
- extensible structure

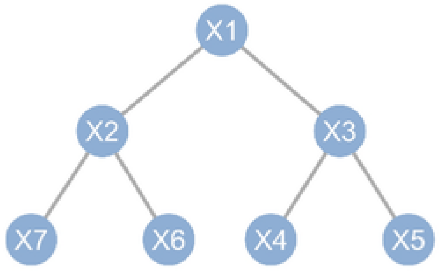

$$\hat{y} = \sum_{k=1}^{n} f_k(x)$$

Energy Flux | **Particle Flux** | **Momentum Flux**

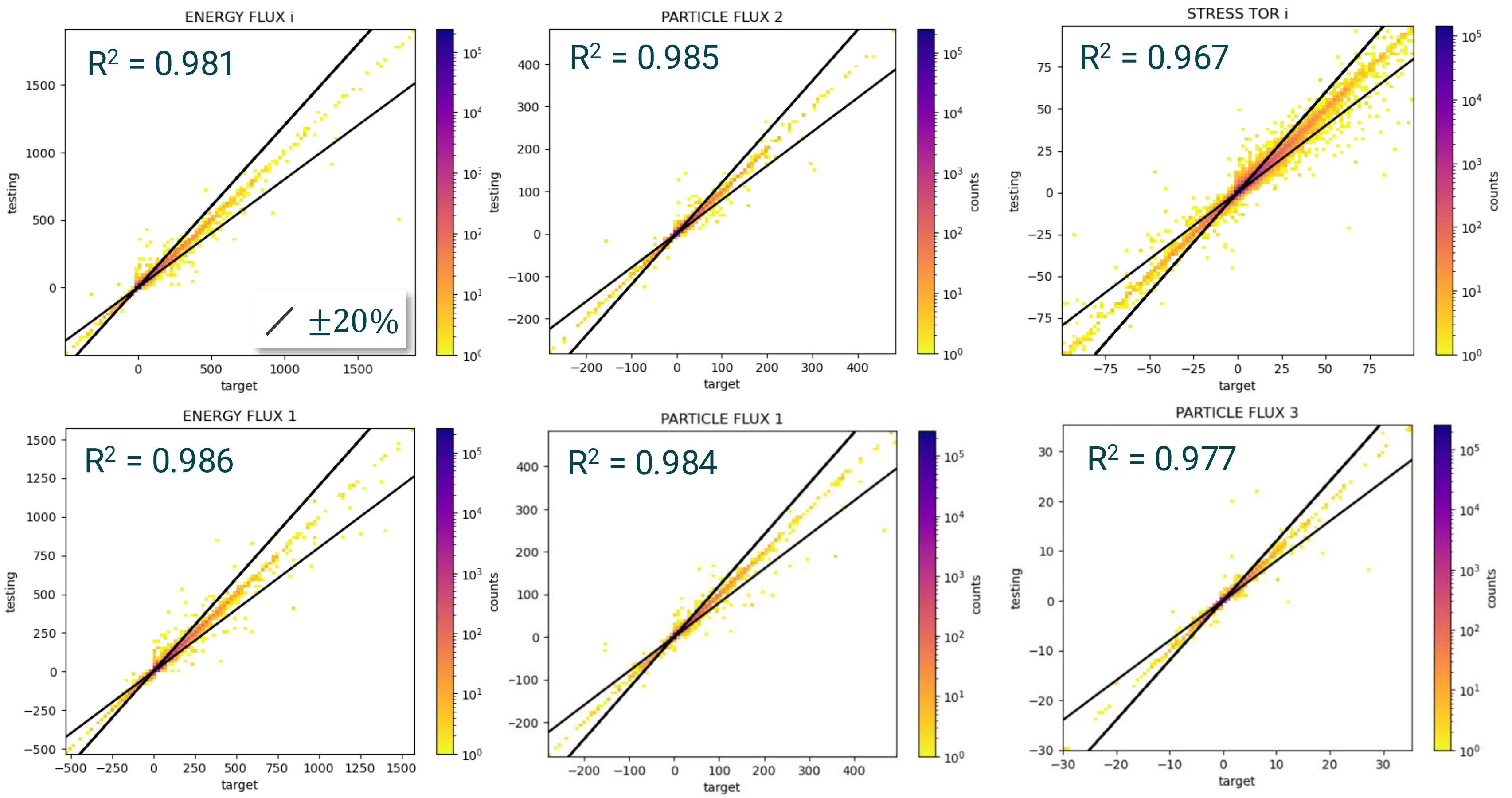

Impurity Flux

*12 branch max depth, 80/20 percent train-test-split

Sensitivity of Surrogate Modeling Framework is Captured by Computationally Tractable Calculation Over Large Datasets

Shapley values: game theoretic description of importance distribution over possible features

1. additive explanation of each parameter for each prediction
2. interaction of each parameter to overall model behavior
3. dominant feature selection for each independent output

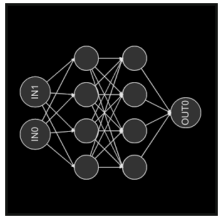

interpretable

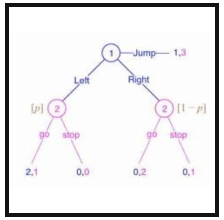

Neural Network **Decision Tree**

Ion Momentum Flux

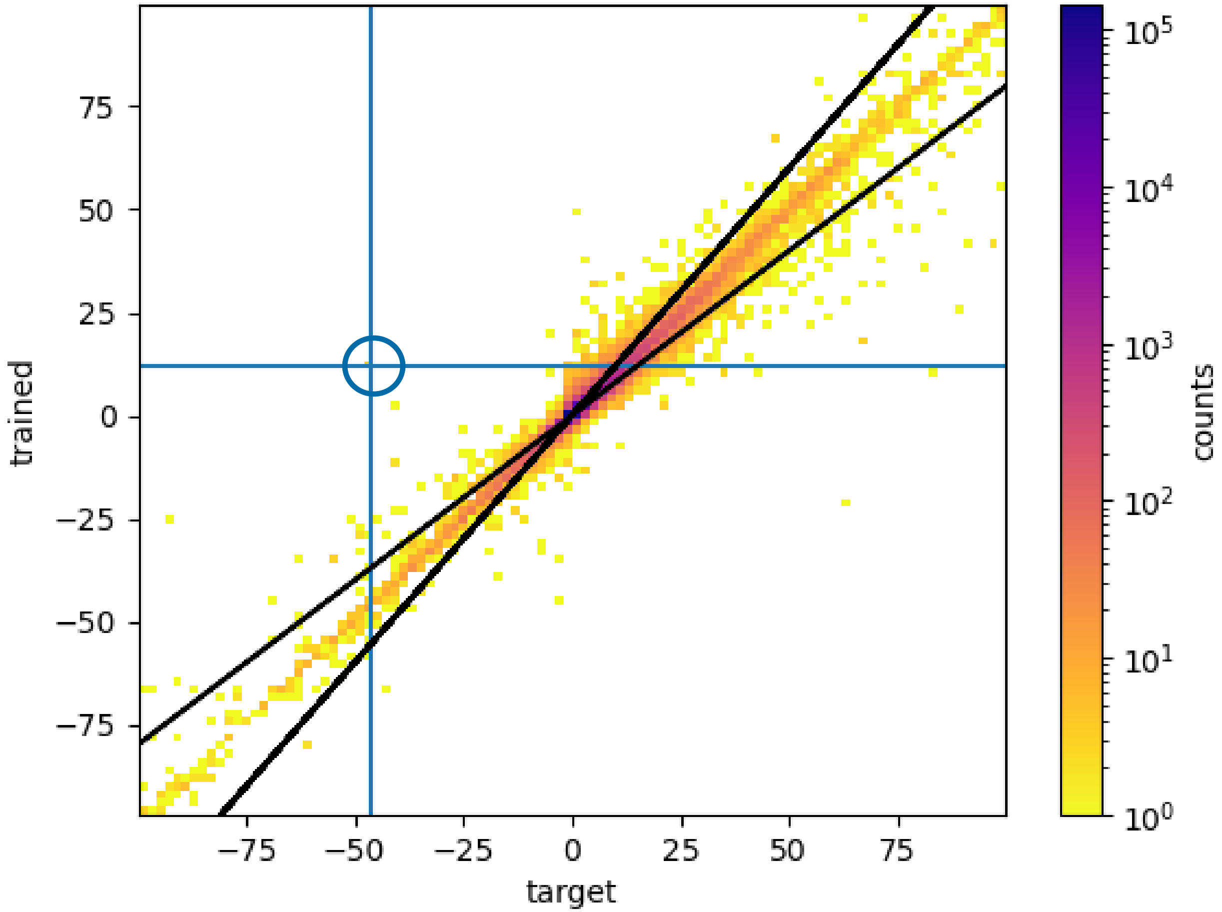

OAK RIDGE National Laboratory

Target Predictions are Evaluated in Terms of Parameter Marginal Contributions Across All Possible Coalitions

Outlier Model Prediction

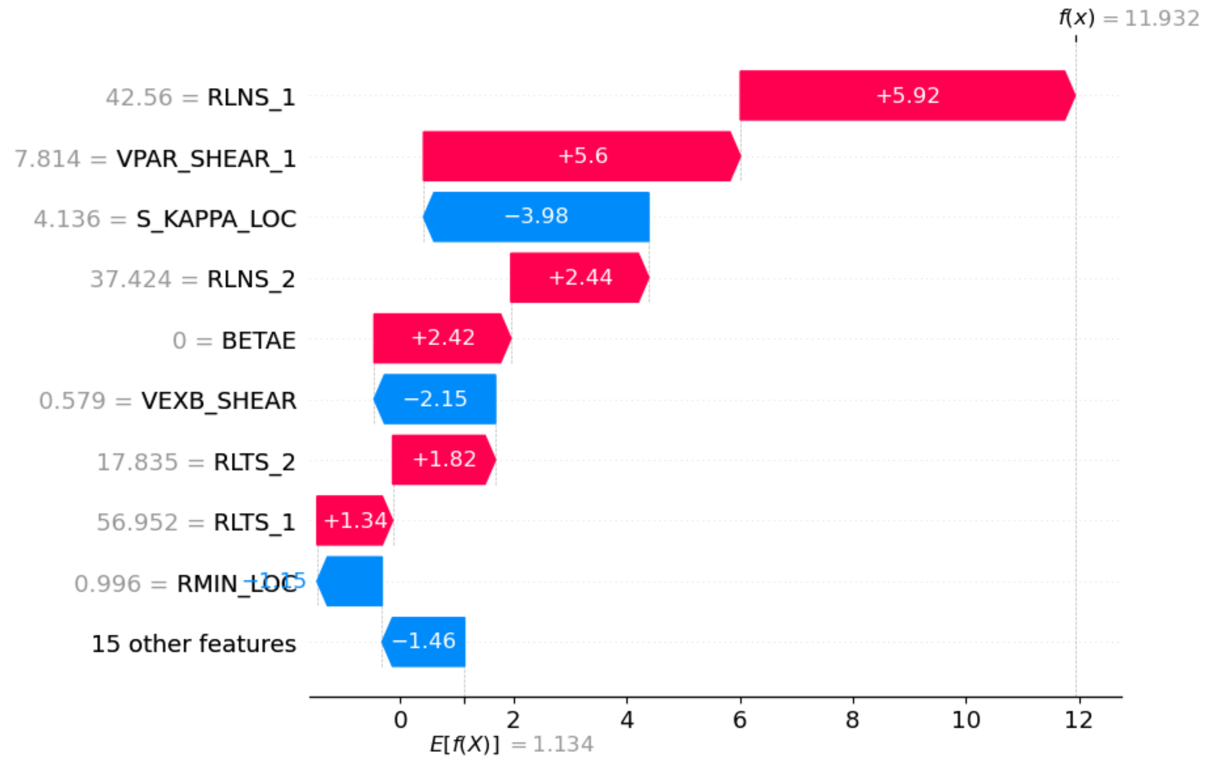

Matched Model Prediction

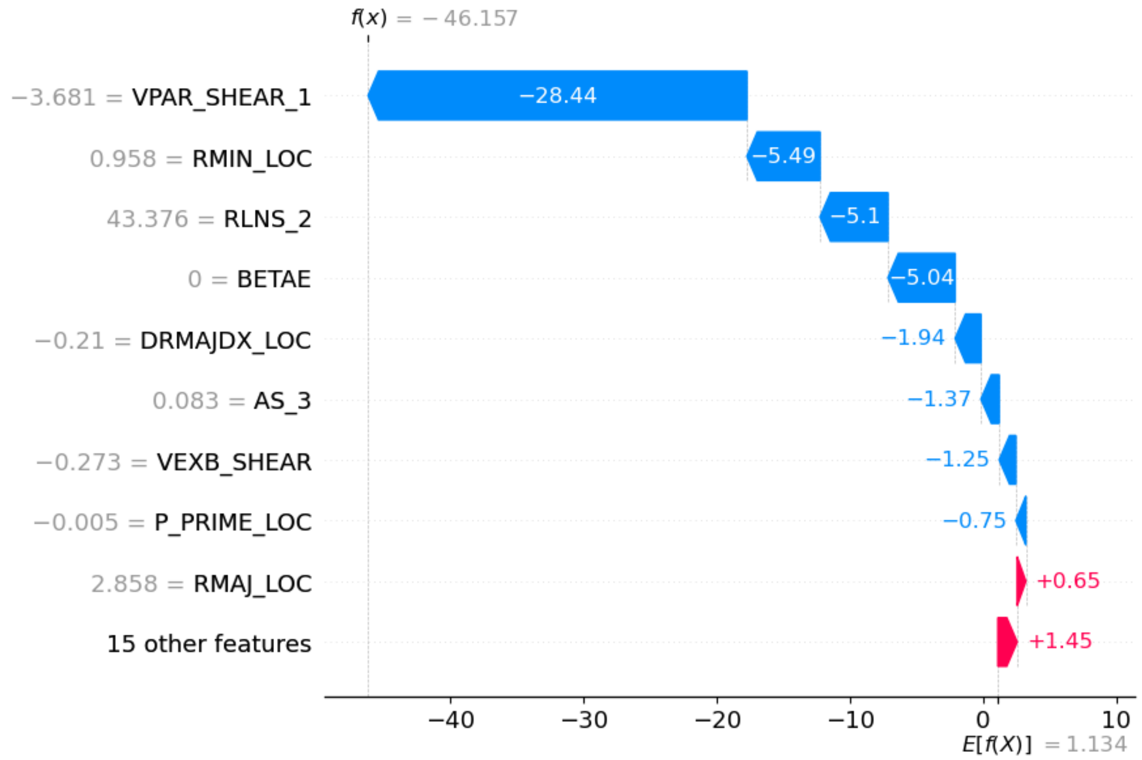

Predictions exhibit contrasting **characteristic response** to model input parameters

Transport Simulations Can be Augmented with Expanded Search Around Particular Coordinate Set Combinations

3 Neighbors Identified as Outliers

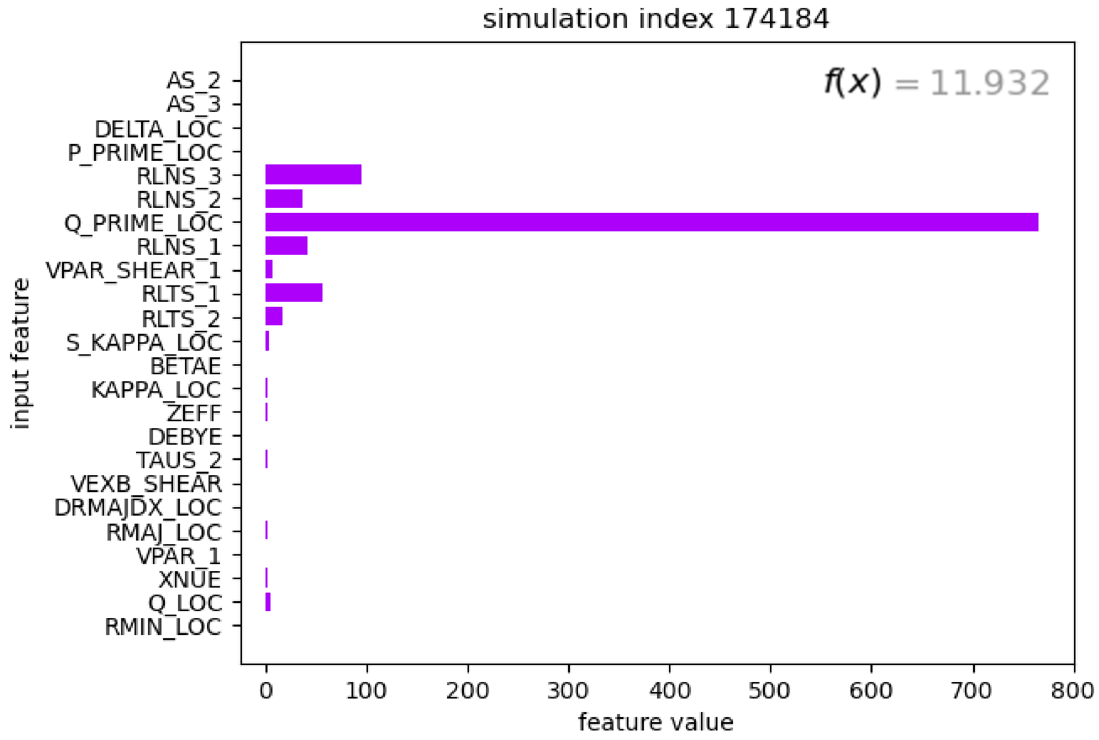

52 Neighbors within 10% of Target

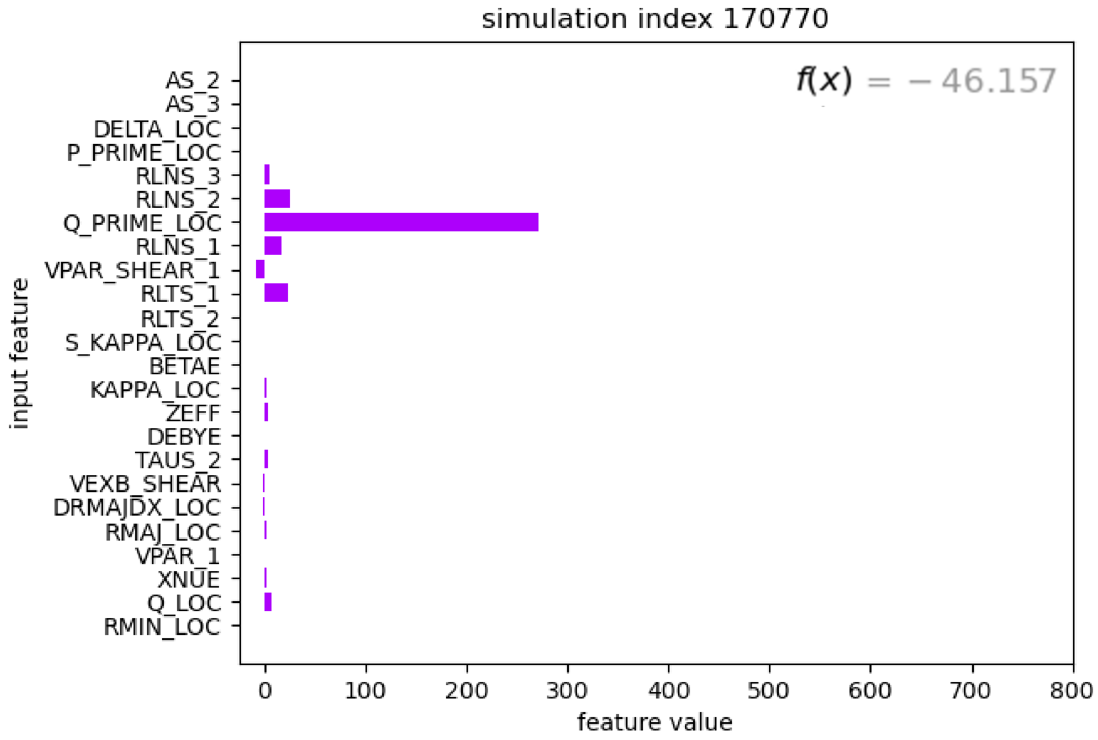

Simulations **sparsely cover** proximal experimental conditions near extrema

Survey of Database Indicates Parameter Interaction Strengths In Terms of Degree and Direction of Model Importance

Ion Momentum Flux

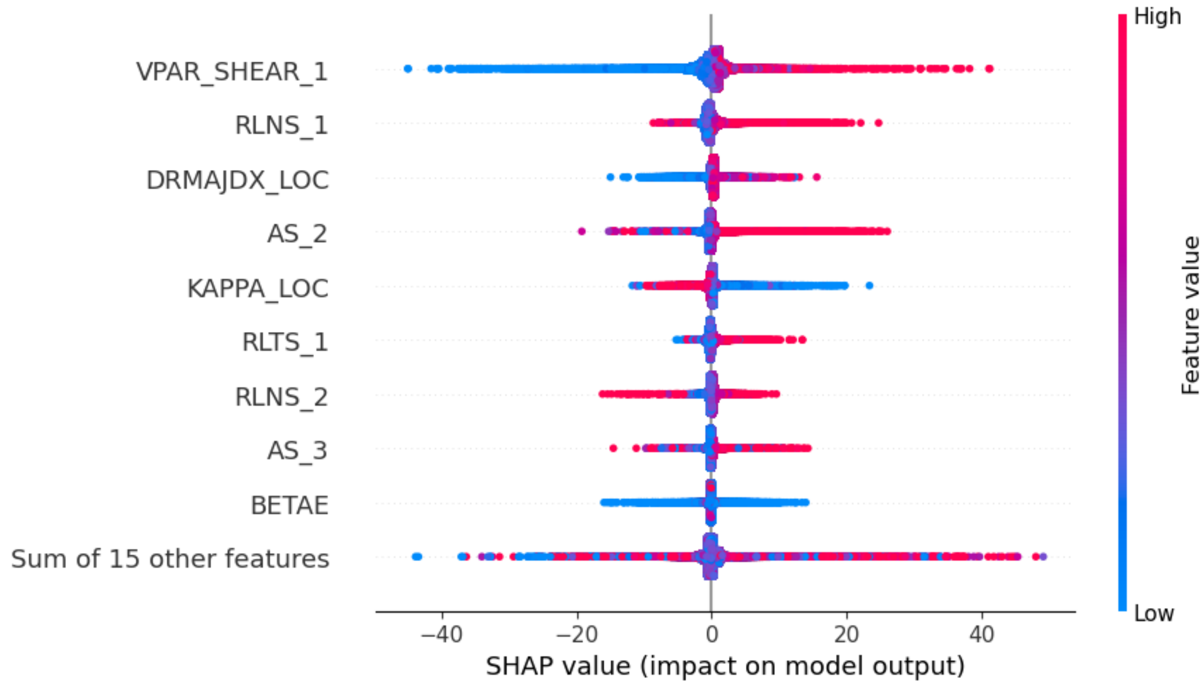

Ion Energy Flux

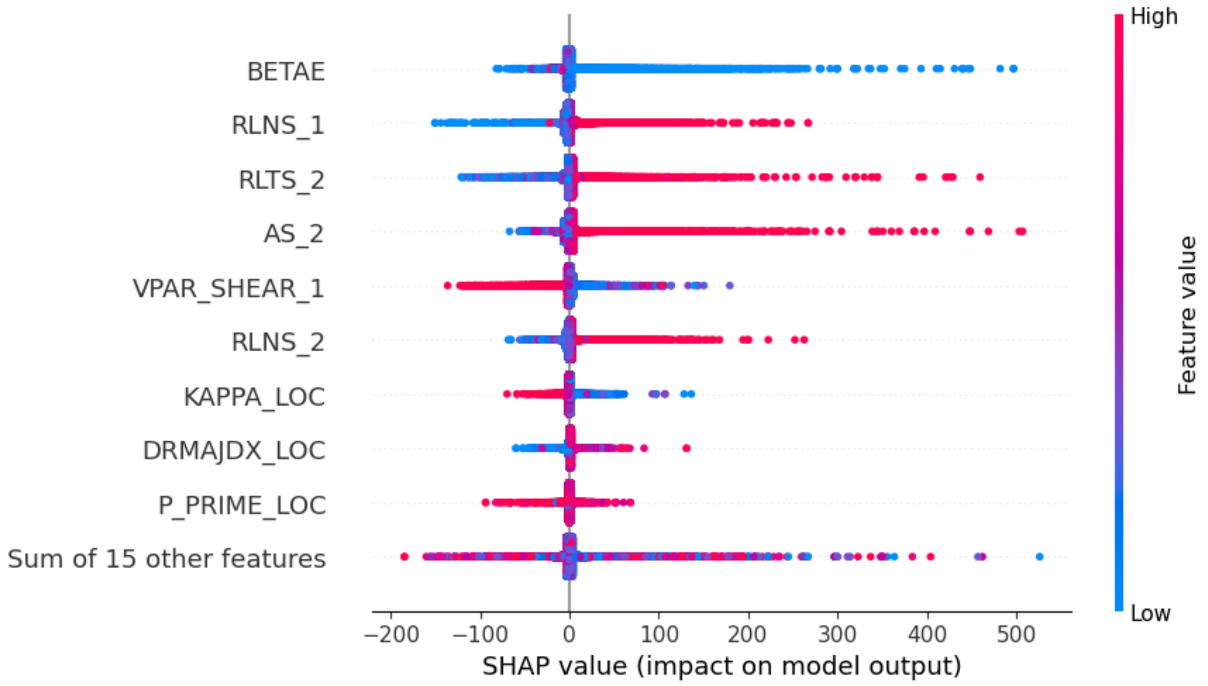

Model sensitivity reveals **significant partial populations** providing minimal impact

Oak Ridge National Laboratory

Explainable Machine Learning Unlocks Physical Insight to Determine Parameter Interdependence for Efficient Sampling

Decoupled Dominant Features

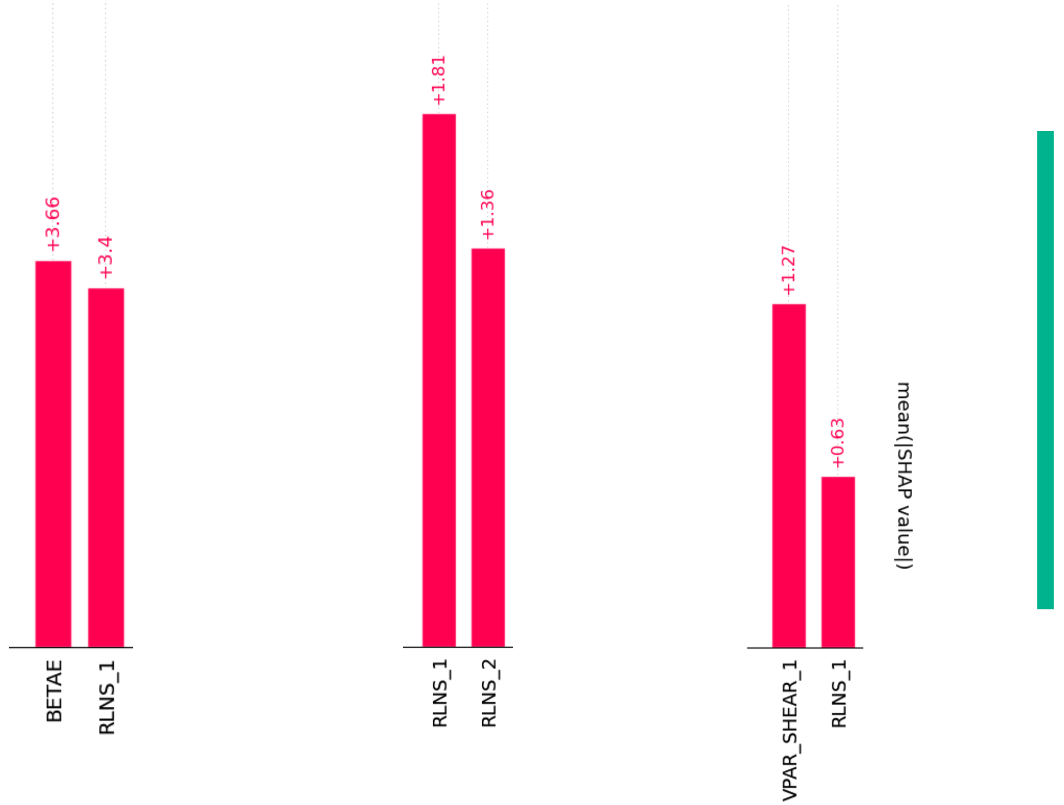

Ion Energy Flux **Ion Particle Flux** **Momentum Flux**

Paired Model Contributions

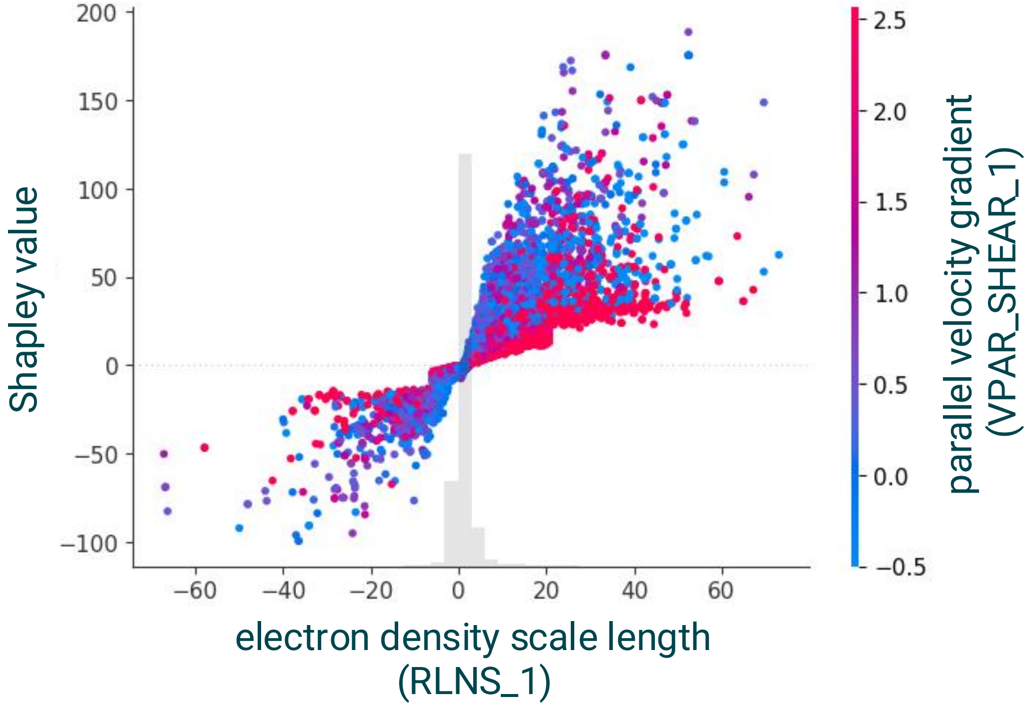

Electron Particle Flux

*see M. Landreman et al., 2025 arXiv:2502.11657 for extensive application to stellarator transport simulations

Explainable Machine Learning Unlocks Physical Insight to Determine Parameter Interdependence for Efficient Sampling

Total Parameter Contributions

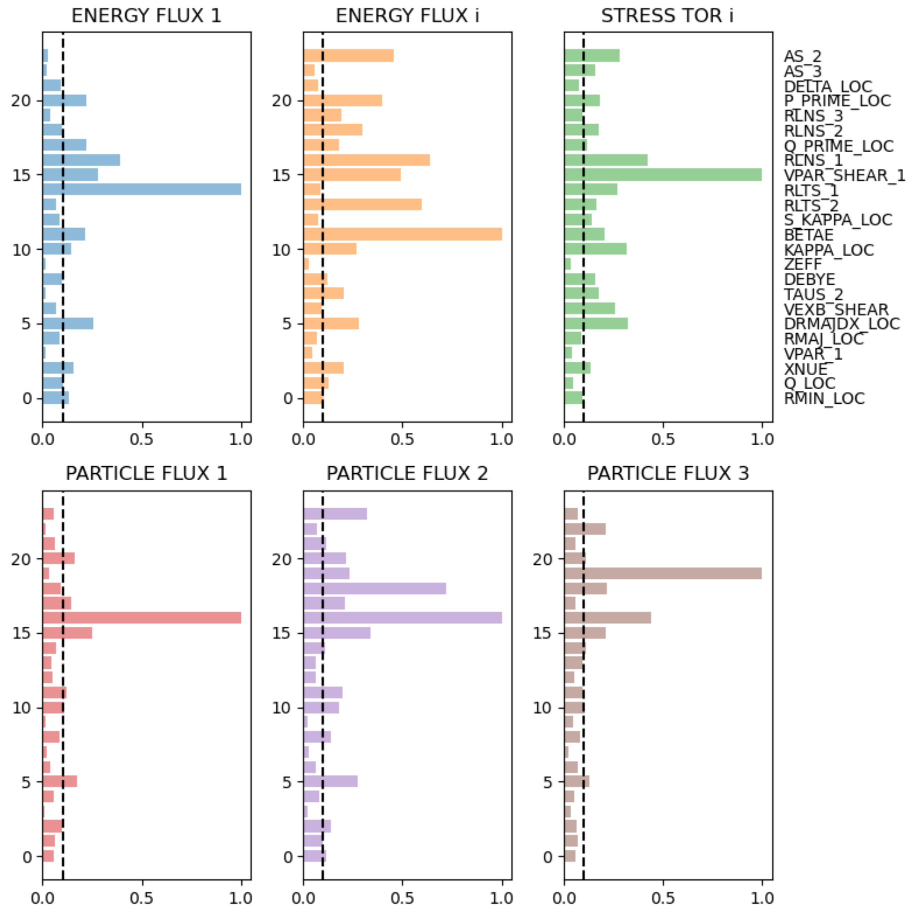

Shapley Value Assessment

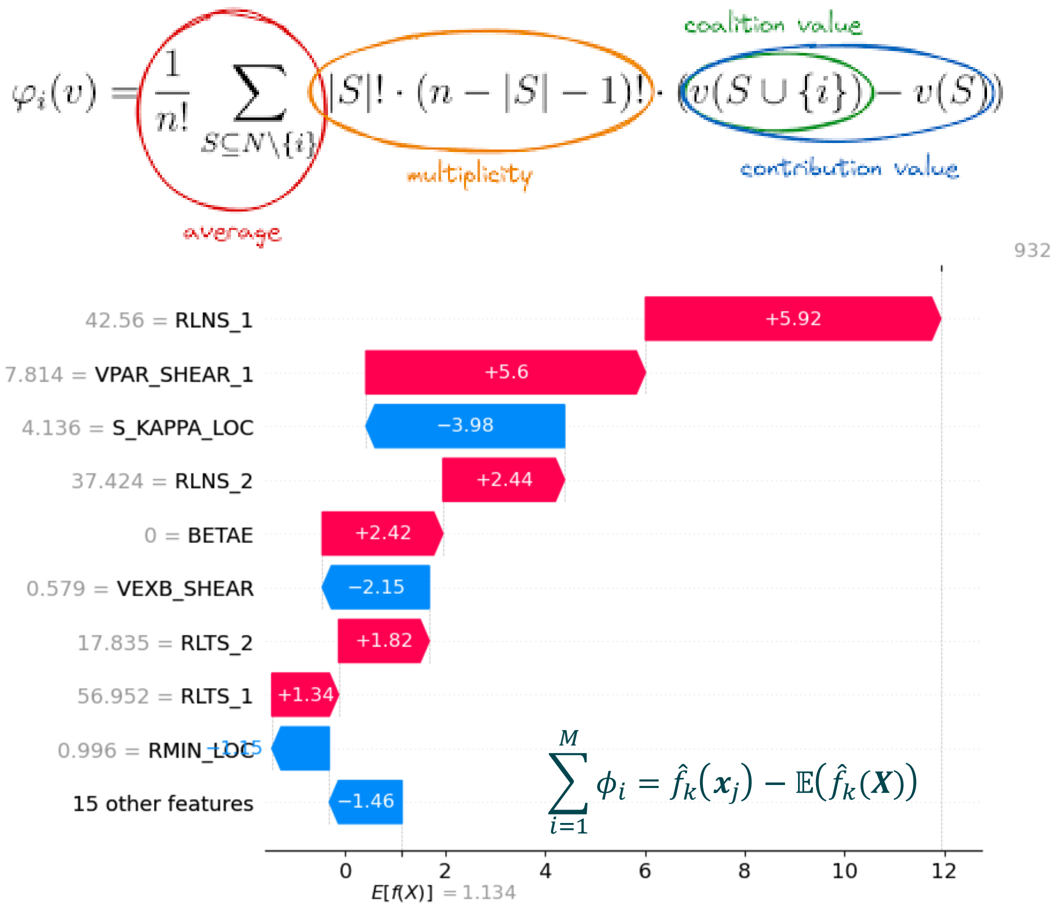

*see M. Landreman et al., 2025 arXiv:2502.11657 for extensive application to stellarator transport simulations

Drastic Reduction in Degrees of Freedom by Feature Importance Sampling of Surrogate Model Shapley Values

24 Input Components

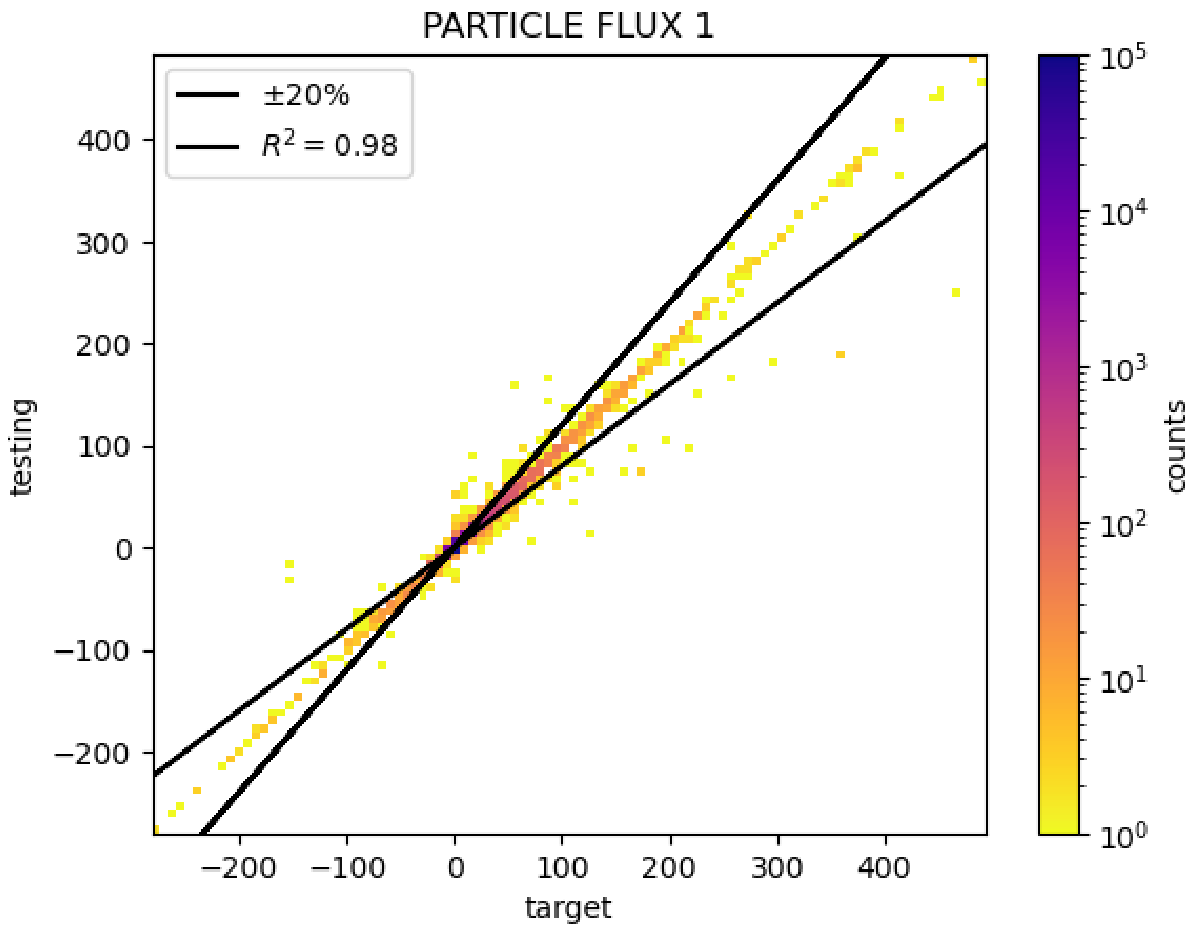

4 Input Components Selected by Shapley

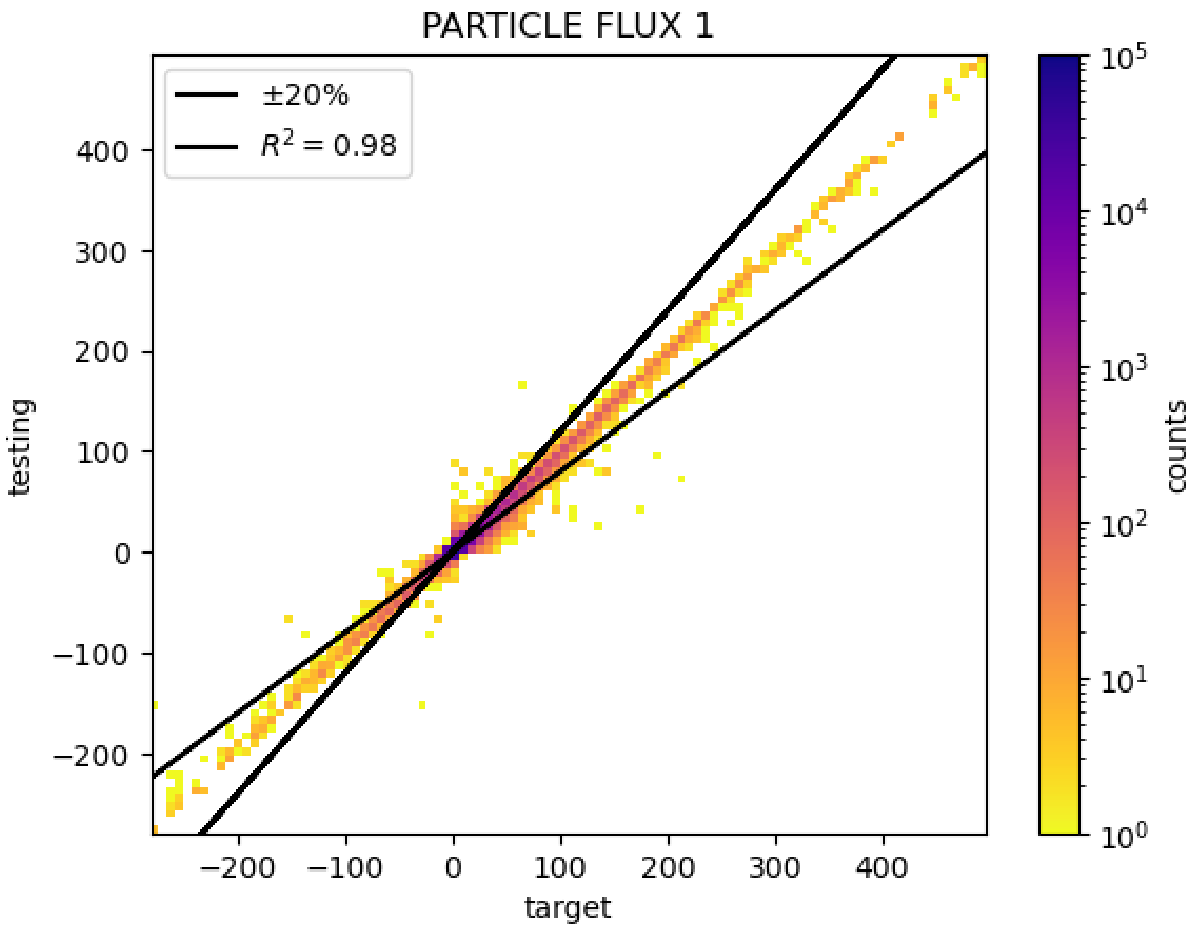

Similar Studies Provide Data-Driven Insight from Machine Learning on Stellarator Turbulent Transport Configurations

Shapley Value Parameter Contribution

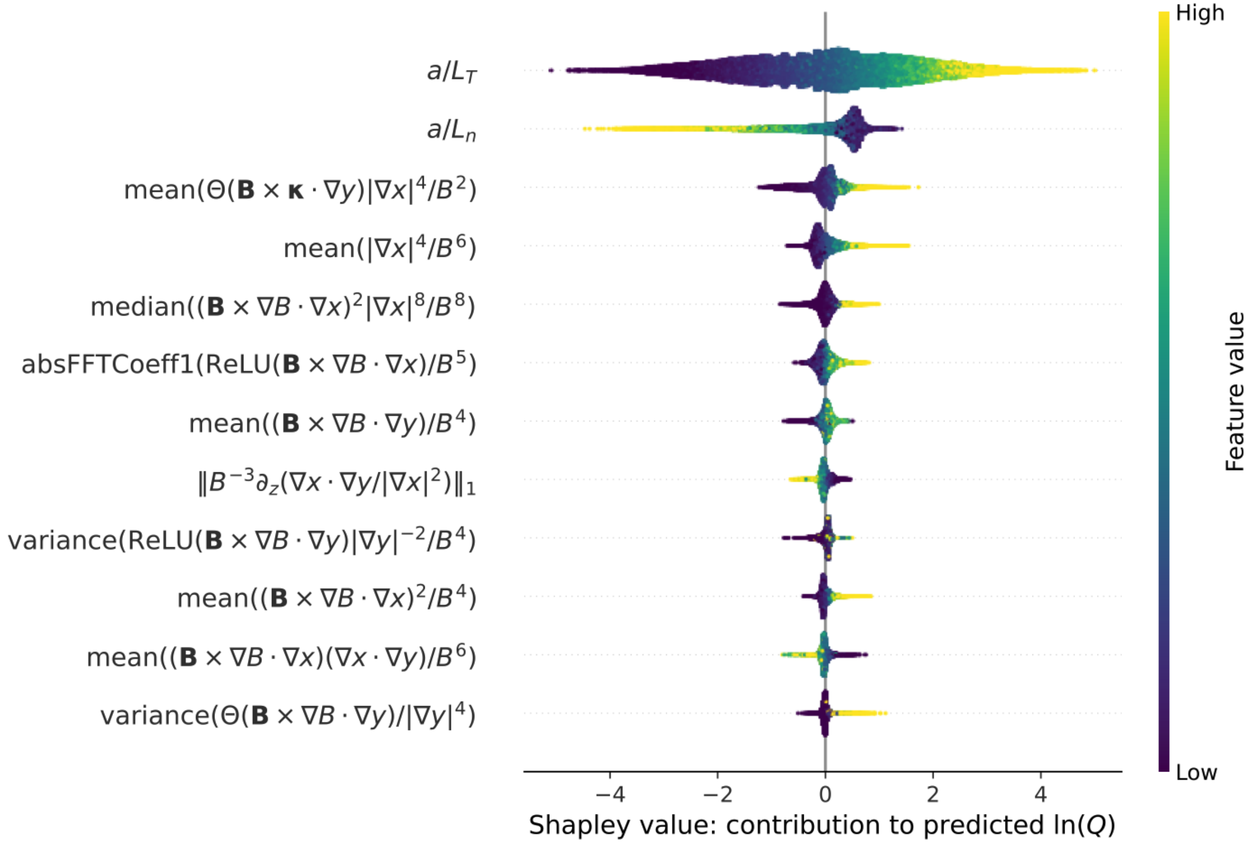

Quasi-Axisymmetric Configurations

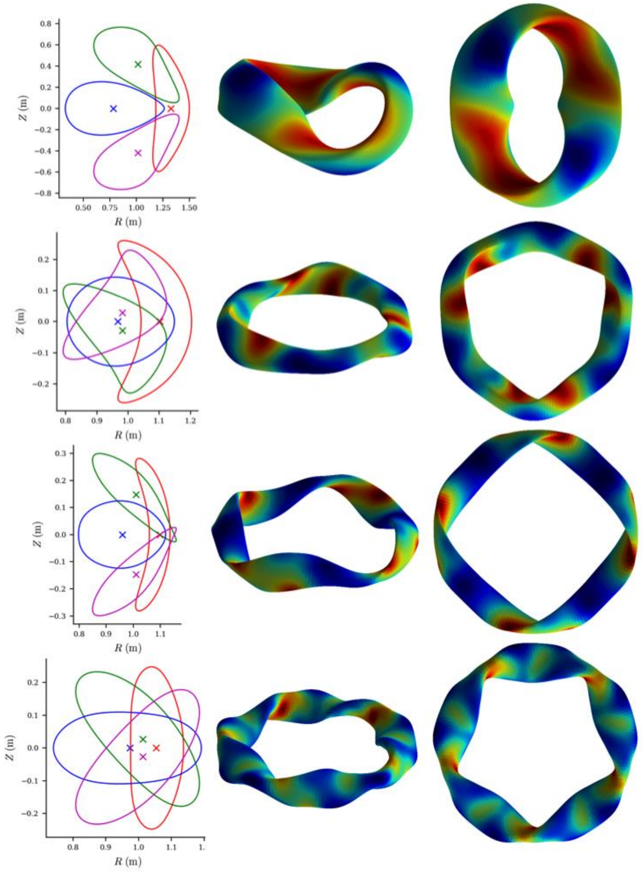

Landreman et al., (2025), arXiv: 2502.11657, *ITG only

Taking Interpretable Machine Learning One Step Further

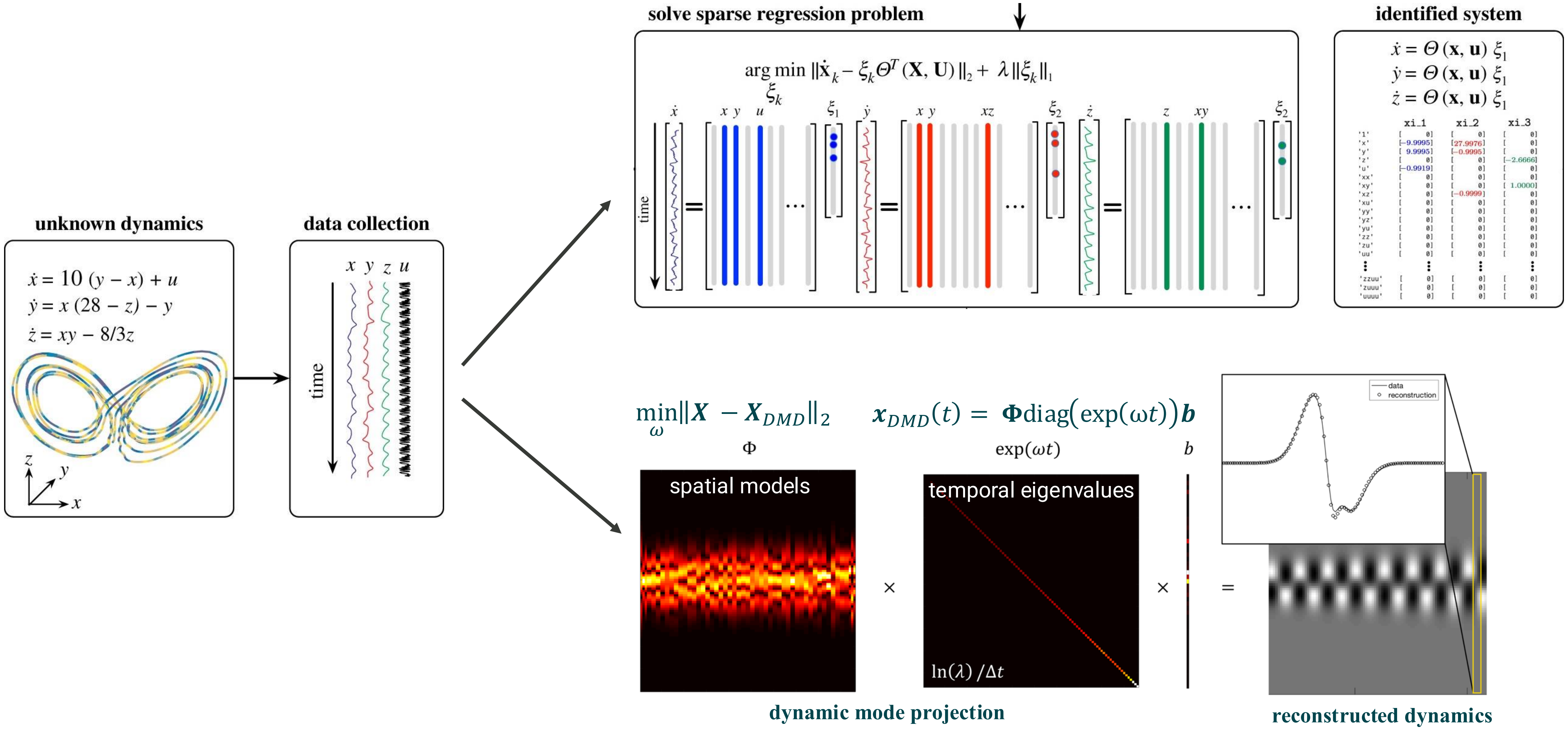

* Adapted from [Kaiser, et al., 2018], Available on Github at /dynamicslab/PySINDy & /PyDMD

Oak Ridge National Laboratory

Operational Performance Can be Governed by Key Observable Quantities Linking Actuators to Divertor Targets

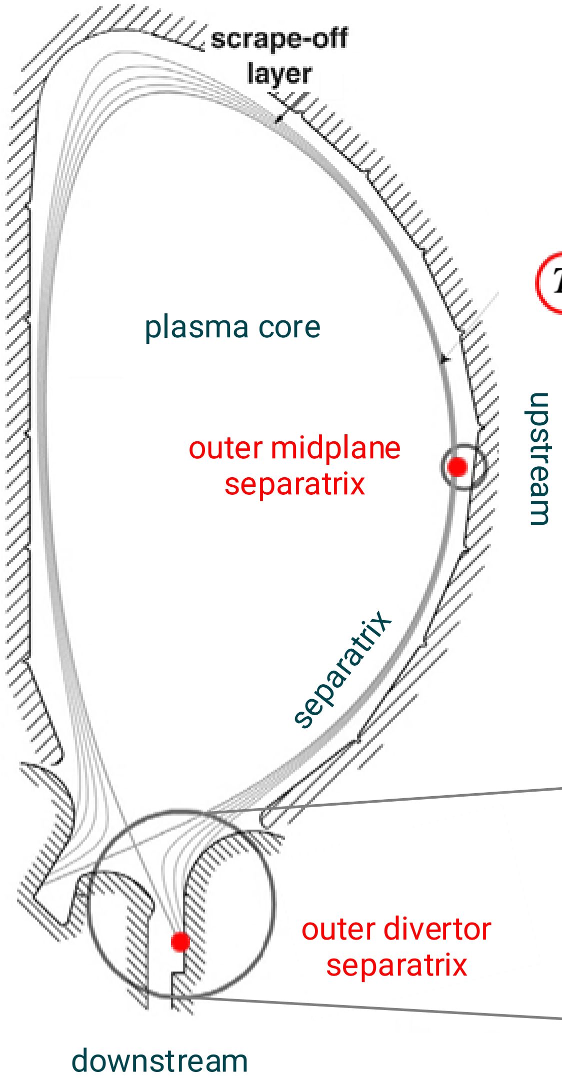

Two-Point Model

$$T_{\mathrm{et}} = \left[\frac{2m_{\mathrm{f}}}{e^3\gamma^2}\left(\frac{2\kappa_{0\mathrm{e}}}{7}\right)^{4/7}\right]\left[\frac{q_{||\mathrm{u}}^{10/7}}{n_{\mathrm{u}}^2 L^{4/7}}\right] \times \left[\frac{(1-f_{\mathrm{cooling}})^2}{(1-f_{\mathrm{mom\text{-}loss}})^2}\right] \quad (\mathrm{eV}),$$

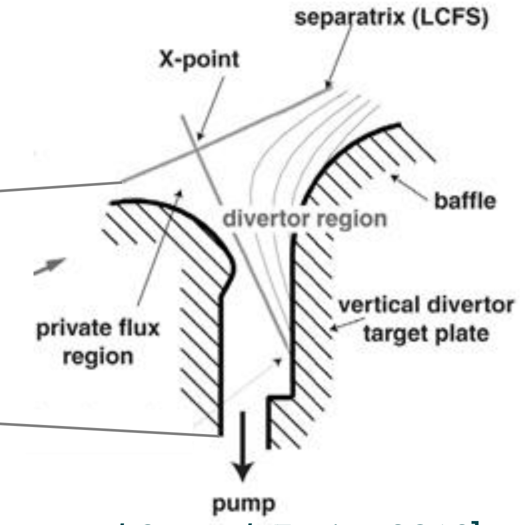

Stangeby, *Plasma Phys. and Control. Fusion* 2018]

Gas Puff Response

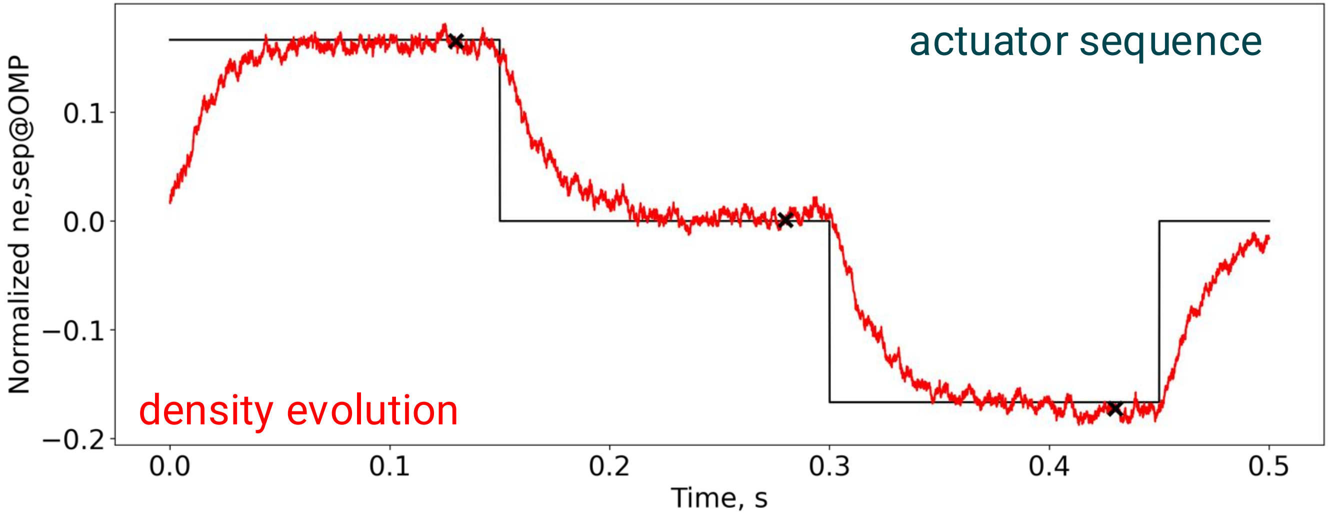

Separatrix values of n_e and T_e exhibit rise and fall times on the order of ~60 – 70 ms with step gas puff actuation

- Preliminary investigation of DIII-D shots shows timescales on the order of ~50 – 100 ms
- First-order Dead Time (FODT) linear fit shows minimal delay in simulated plasma response to direct actuation

❑ De Pascuale et al., Phys. Plasmas, 2022
https://doi.org/10.1063/5.0110393

Dynamics are Best Characterized by Inverse Dependence of Key Plasma State Variables on Outer Divertor Target

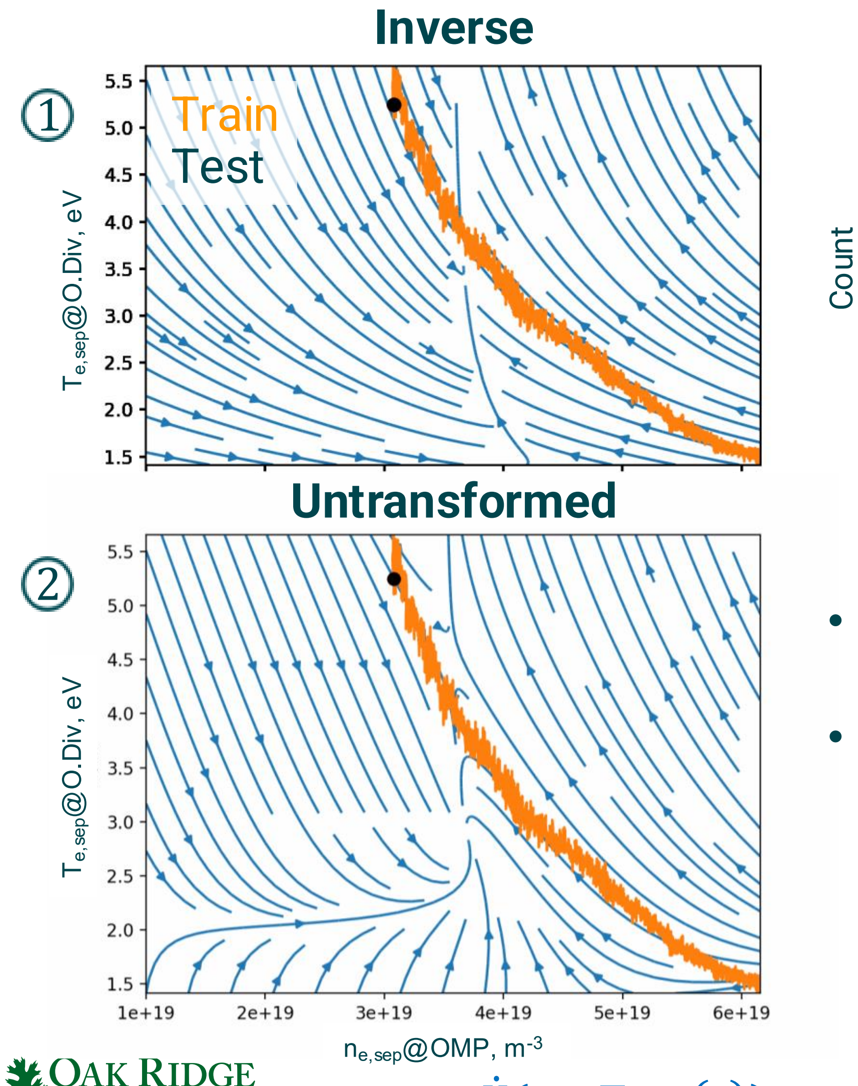

$\dot{X}(n_0, T_0, u(t))$

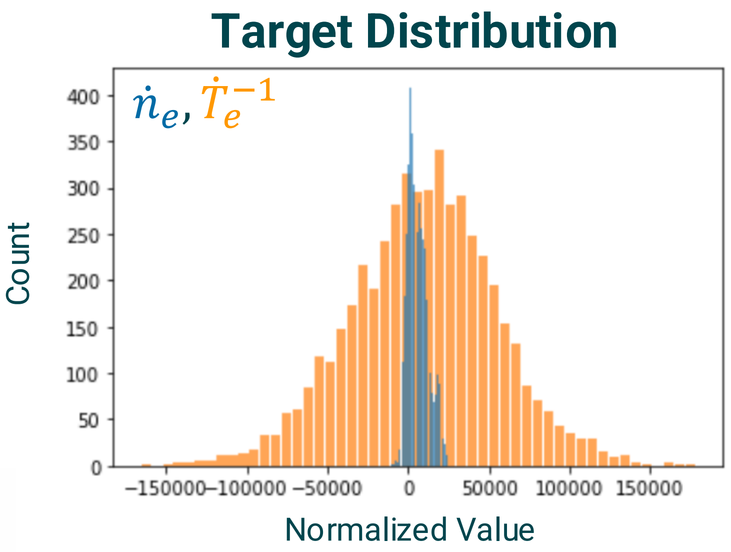

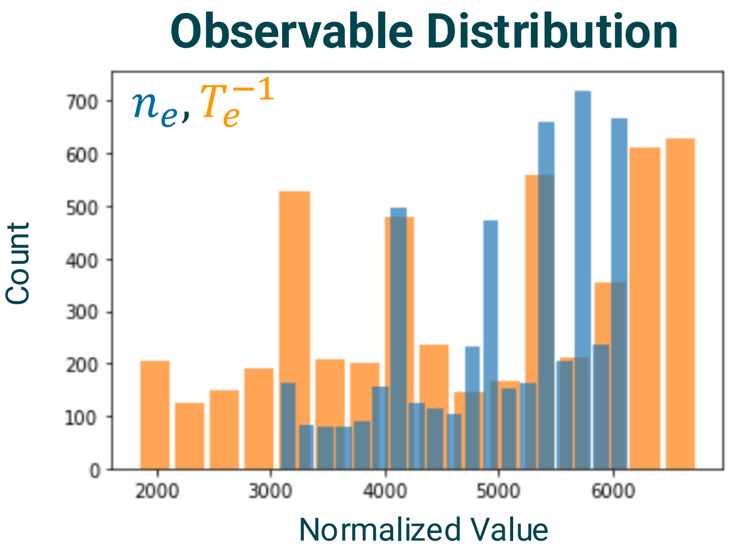

- Data rescaling allows for physically consistent exploration of input parameter space for determination of controlled trajectories
- Identified coupled nonlinear equations are not sparse, but can be analyzed for stability characteristics to prevent over-fitting

❑ Lore et al., Nucl. Fusion, 2023
https://doi.org/10.1088/1741-4326/acbe0e

OAK RIDGE National Laboratory

Integration of Workflow Demonstrates Unique Capability for Evaluation of Strategies for Performance Optimization

Target Setpoint

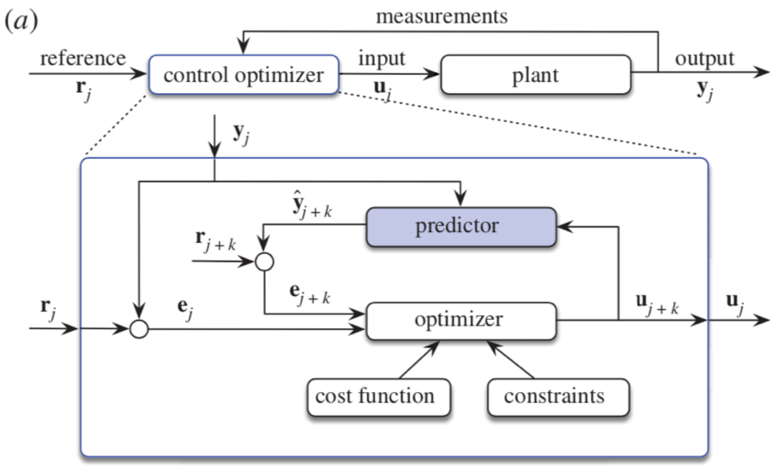

Process Variables

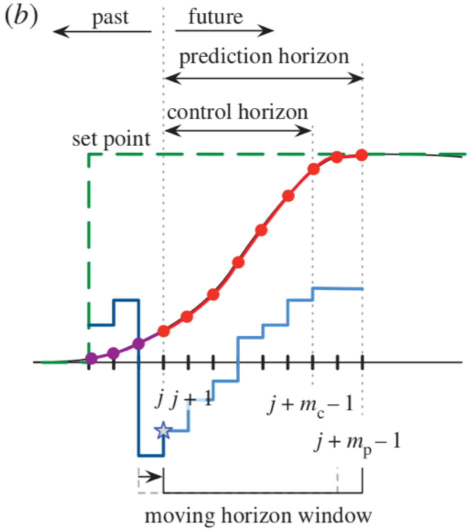

IPS-FASTRAN Implementation

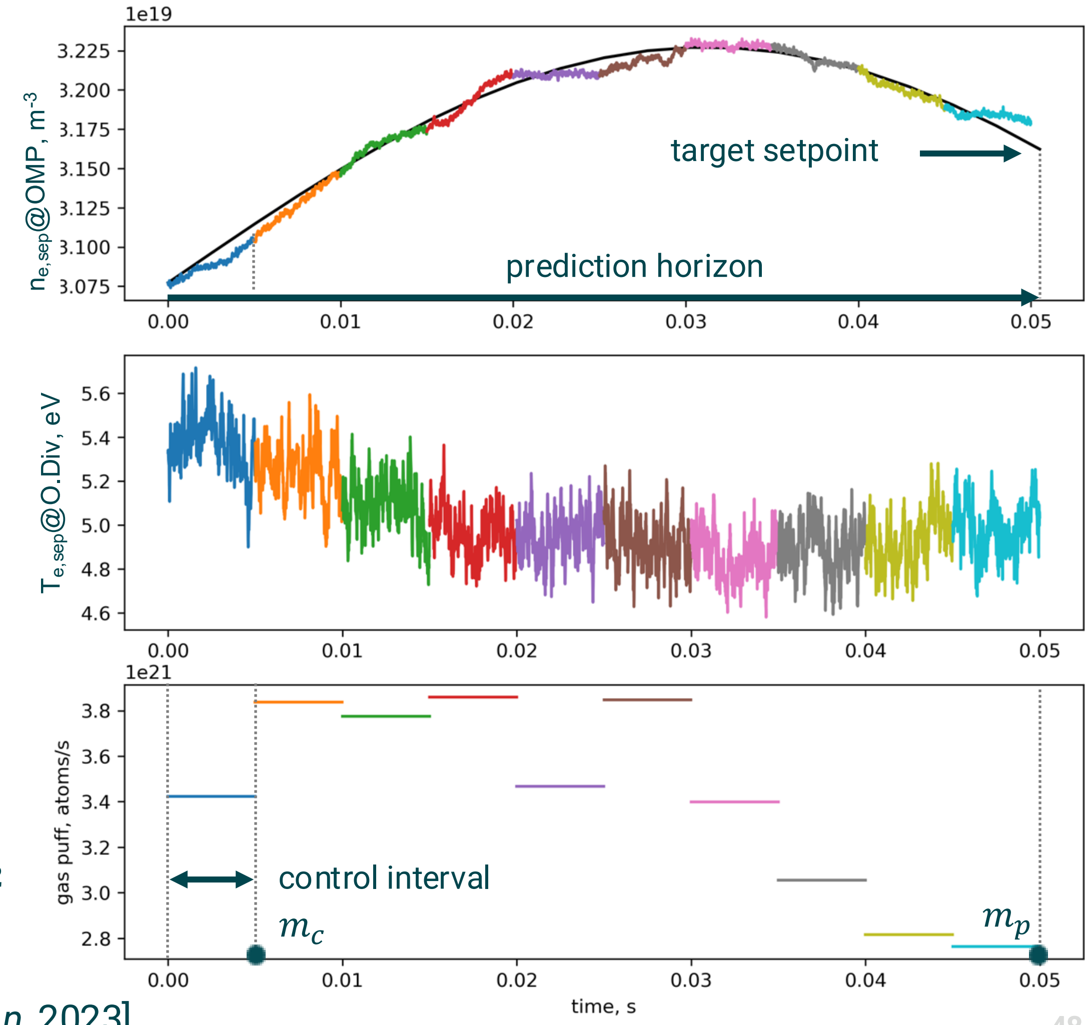

- Model predictive control minimize cost function subject to constraints on input and output quantities
- IPS-FASTRAN provides framework for SOLPS-ITER runs with feedback from extracted reduced models

$$J = \left\| x_{j+m_p} - \tilde{x}_{m_p} \right\|^2 + \sum_{k=0}^{m_p-1} \left\| x_{j+k} - \tilde{x}_k \right\|^2 + \sum_{k=1}^{m_c-1} \left\| u_{j+k} \right\|^2 + \left\| \Delta u_{j+k} \right\|^2$$

[Kaiser, et al., *Proc. Royal Soc. A.* 2018]; [Lore, et al., *Nucl. Fusion*, 2023]

Science Highlight from SULI Program Internship – A. Irvin (UTK)

Scientific Achievement

- Surrogate model accelerates FPP design and optimization of plasma profile control system utilizing electron cyclotron heating and current drive
- 25x reduction in compute time to generate electron cyclotron heating and current drive profile predictions based on 9 free parameters

Significance and Impact

- Surrogate model of TORAY ray tracing code provides rapid predictions with uncertainty quantification
- Inverse-solvable model can predict inputs needed to generate a desired output without the need for large parameter scans for rapid optimization

Research Details

- Former SULI/ECO internship (E. Hassan and S. De Pascuale) and current UT-Knoxville graduate student assistantship (L. Casali)
- Regression using database of 1600 points for a compact advanced tokamak (CAT) using IPS-TokDesigner

- ❑ Irvin et al., Fus. Sci. and Tech., 2025 https://doi.org/10.1080/15361055.2025.2476829

Advance Tokamak

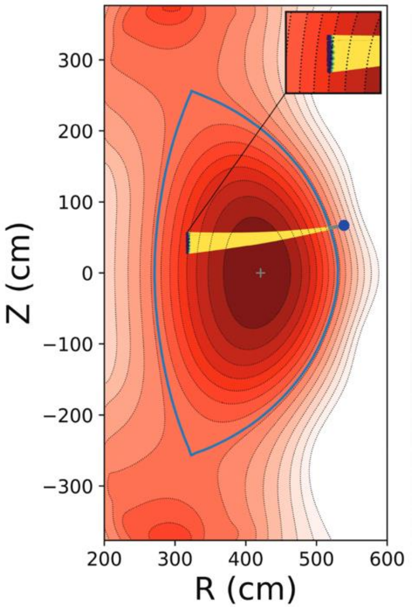

Ensemble Simulations

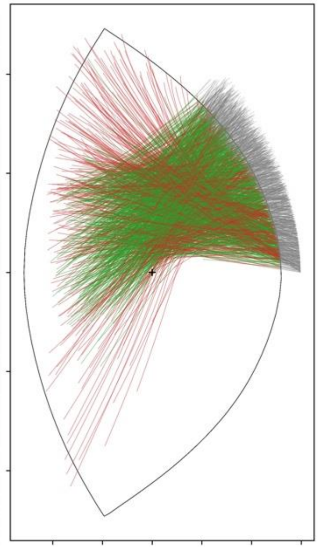

Predicted Profiles

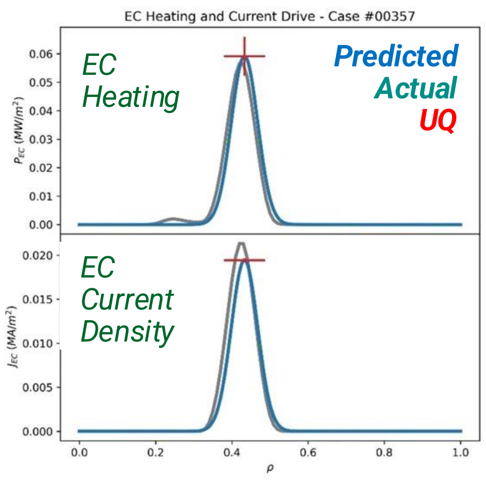

Parameter Regression

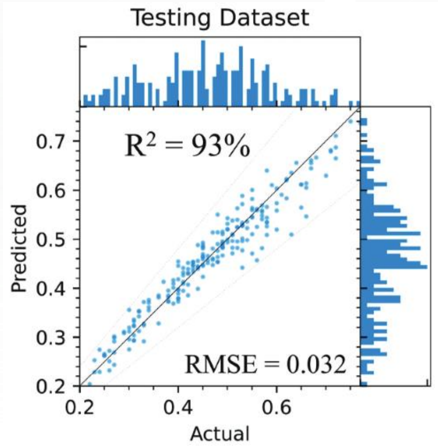

Inverse Modeling

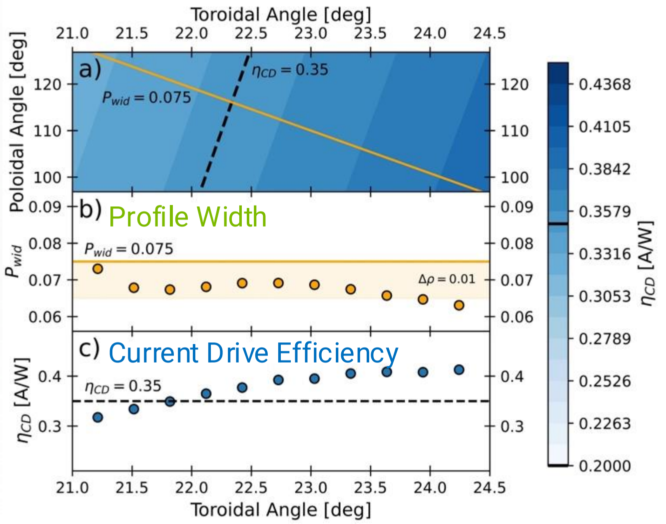

Three Takeway Themes

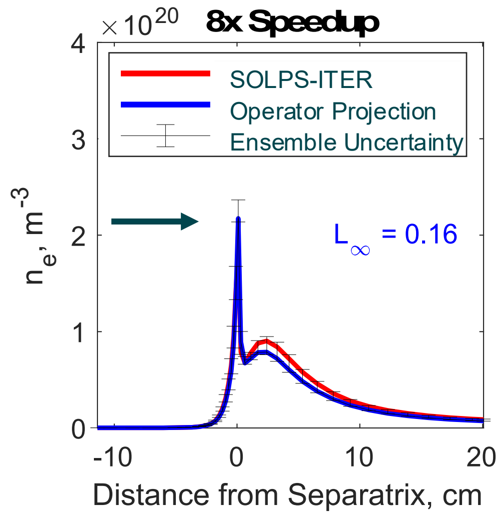

Reduced Modeling

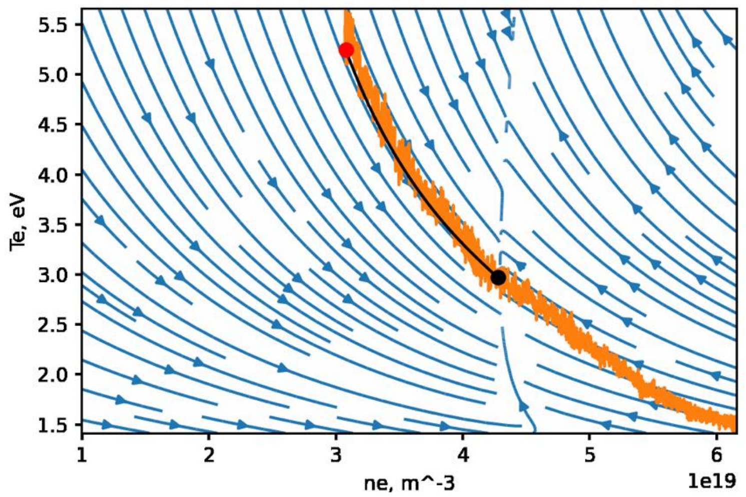

Sparse Optimization

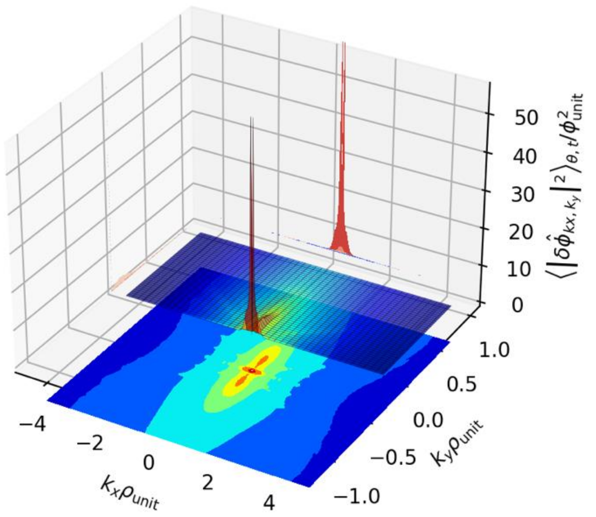

Machine Learning

$$x_{k+1} = \boldsymbol{A}x_k$$

$$x_{k+1} = \boldsymbol{A}x_k + \boldsymbol{B}u_k$$

$$\frac{dx}{dt} = \sum_{i=0}^{3}\sum_{j=0}^{3} a_{ij}x^i u^j$$

$$\frac{dy}{dt} = f\left(\sum_{i=1}^{n} x_i w_i + b_i\right)$$

Oak Ridge National Laboratory

The Integrated Plasma Simulator (IPS) Framework is Enabling Surrogate Model Development for Online Coupled Workflows

- **Accelerate** expensive simulation of core transport and pedestal stability within a coupled framework
- **Predict** plasma boundary response to core and pedestal conditions during detachment control
- **Quantify** uncertainty in machine learning surrogate models for decision-ready tokamak pulse simulation

These aims enable fast tokamak pulse simulation for:

1. **Reactor design** leveraging physics informed and Bayesian inference neural networks to reduce dimensionality of coupled simulations
2. **Session planning** leveraging data assimilation and adaptive sampling to constrain predictions of operational space

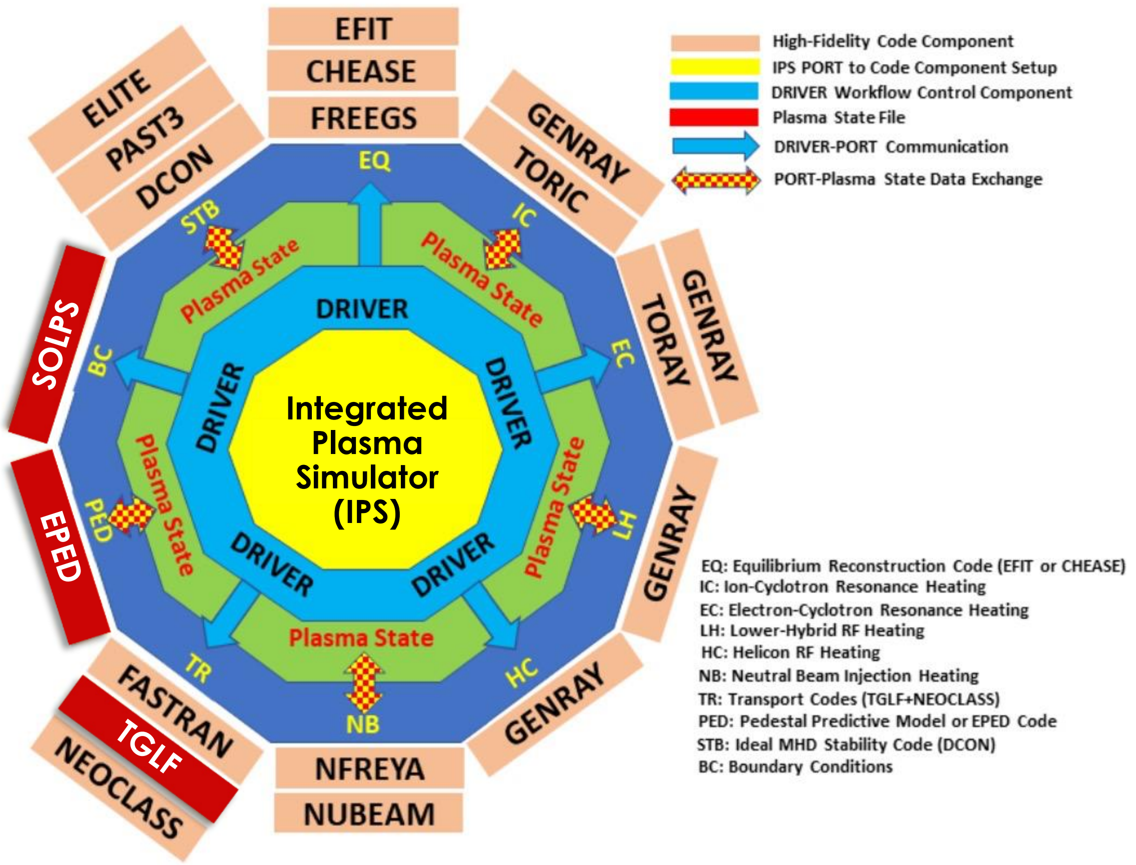

Multi-Fidelity Model Coupling Framework

*Adapted from Hassan et al., (2023), *FST*, 79, 189

Code-Piloting Advanced Simulations for Reactor Digital Twins

How can we predict anomalous transport in the plasma boundary?

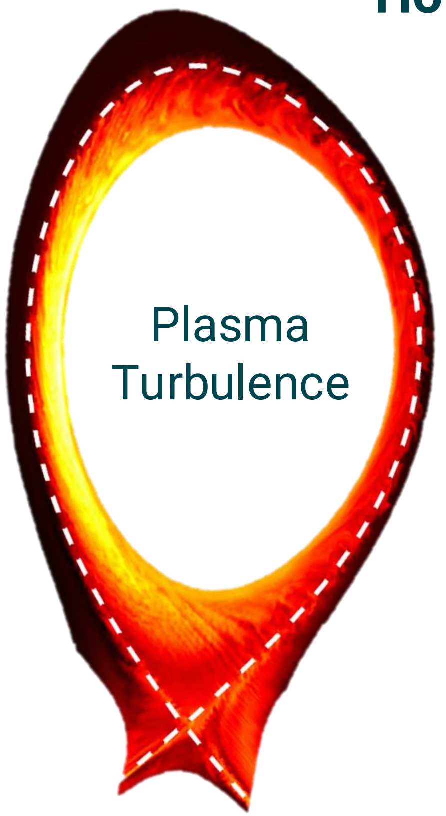

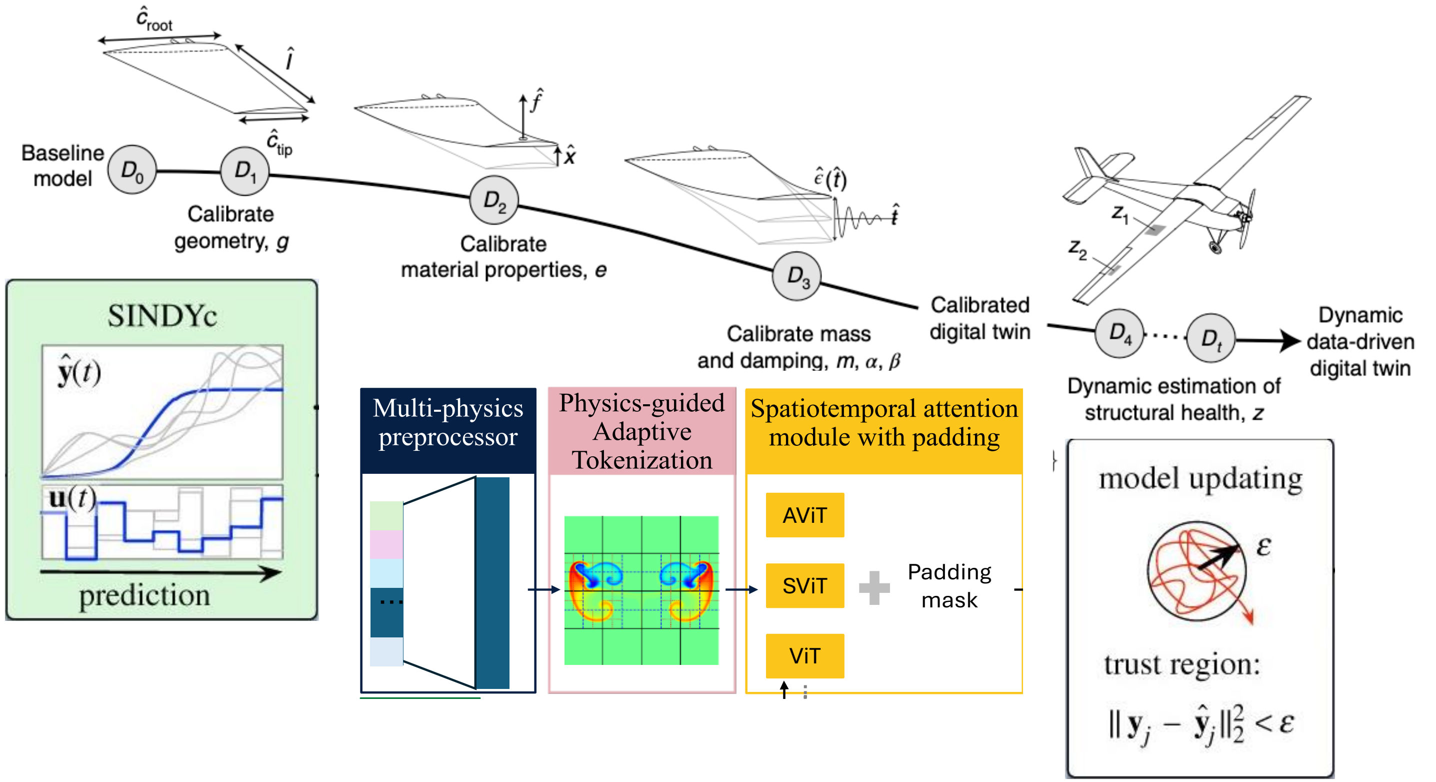

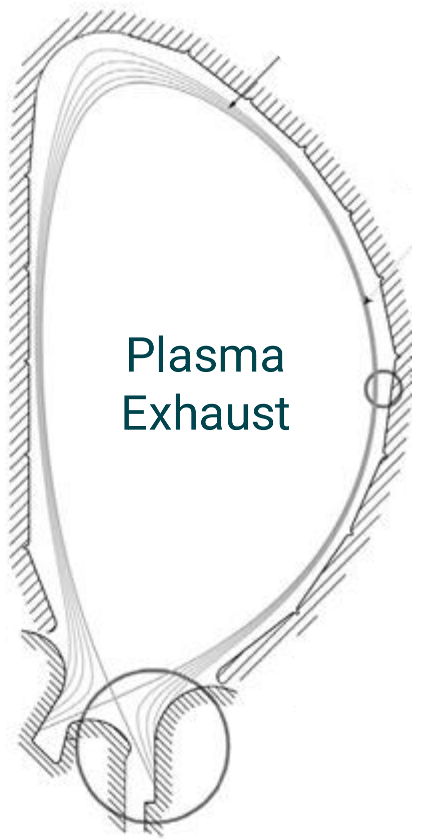

Advanced Profile Prediction for Fusion Pilot Plant Design
PI: D. Ernst at MIT (FIRE 2024 to 2028)

Trustworthy Multiscale Probabilistic Turbulence Foundation Models
PI: P. Zhang at ORNL (LDRD 2023 to 2026)

$$\Gamma_\perp \propto D_\perp, \chi_\perp \left(\frac{\partial}{\partial r}\right) n, T$$

[Federici, et al., *NF*. 2021; https://arxiv.org/abs/2412.20601]

About You – Where will your science story go from here?

"Remember to look up at the stars and not down at your feet. Try to make sense of what you see and wonder about what makes the universe exist. Be curious" – Stephen Hawking

ITER Tokamak

W7-X Stellarator

"In science, it is not speed that is most important. It is the dedication, the commitment, the interest and the will to know something and understand it" – Eugene Wigner

OAK RIDGE
National Laboratory

OAK RIDGE
National Laboratory

U.S. DEPARTMENT OF ENERGY

ORNL IS MANAGED BY UT-BATTELLE LLC
FOR THE US DEPARTMENT OF ENERGY

Multi-Parameter Mapping of Input Space to Targeted Output Quantities for Reduced Simulation Scans of TGLF Sensitivity

Variable	Definition
r/a	Normalized minor radius
R/a	Normalized major radius
κ	Elongation
$r\frac{\partial\kappa}{\partial r}$	Elongation shear
δ	Triangularity
$\frac{\partial R}{\partial r}$	Shafranov shift
q	Safety factor
$\frac{q^2a^2}{r^2}\frac{\partial q}{\partial r}$	Safety factor shear
β_e	Kinetic to magnetic pressure ratio
ν_{ie}/ac_s	Collision frequency
T_i/T_e	Ion to electron temperature ratio
n_D/n_e	Deuterium to electron density ratio
n_C/n_e	Carbon to electron density ratio
Z_{eff}	Effective ion charge
a/L_{Te}	Electron temperature scale length
a/L_{Ti}	Ion temperature scale length
a/L_{ne}	Electron density scale length
a/L_{nD}	Deuterium density scale length
a/L_{nC}	Carbon density scale length
$\frac{qa^2}{rB^2_{unit}}\frac{\partial p}{\partial r}$	Total pressure gradient
$\text{sign}(I_p)R\omega_{tor}\frac{a}{c_s}$	Parallel velocity
$-\text{sign}(I_p)R\frac{\partial\omega_{tor}}{\partial r}\frac{a}{c_s}$	Parallel velocity gradient
$-\text{sign}(I_p)\frac{r}{q}\frac{\partial\frac{V_{E\times B}}{R}}{\partial r}\frac{a}{c_s}$	$E\times B$ velocity shear

24 Input Dimensions

Energy Flux 1 (6) **Energy Flux 2 (7)**

- VPAR_SHEAR_1
- BETAE
- RLNS_1/2
- RLTS_1/2

Momentum Flux 2 (7+)

- VEXB+SHEAR
- KAPPA_LOC
- P_PRIME_LCO

Particle Flux 1 (6) **Particle Flux 2 (7)** **Particle Flux 3 (6)**

- DRMAJDX_LOC
- VPAR_SHEAR_1
- RLNS_1/2/3
- AS_2/3

Particular Challenge in Capturing Momentum Flux Variability

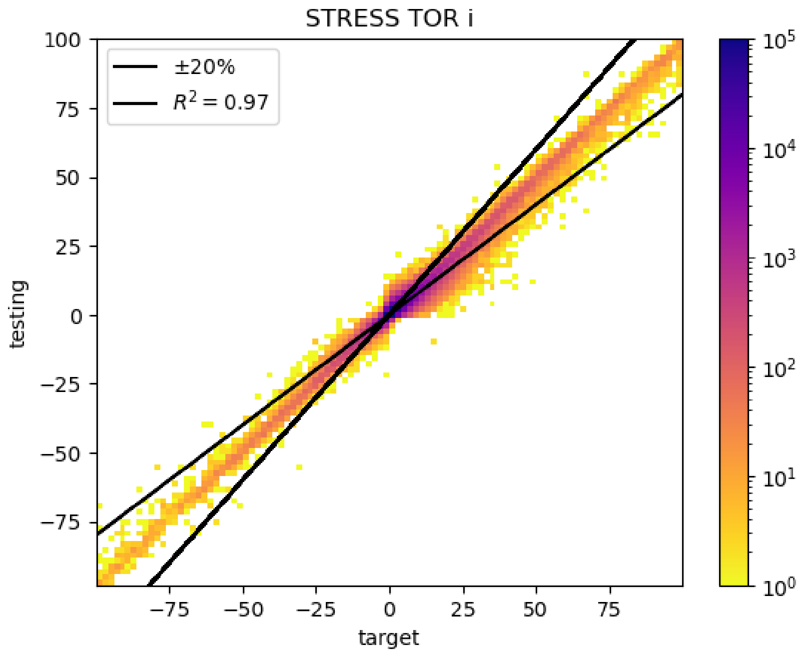

7 Components

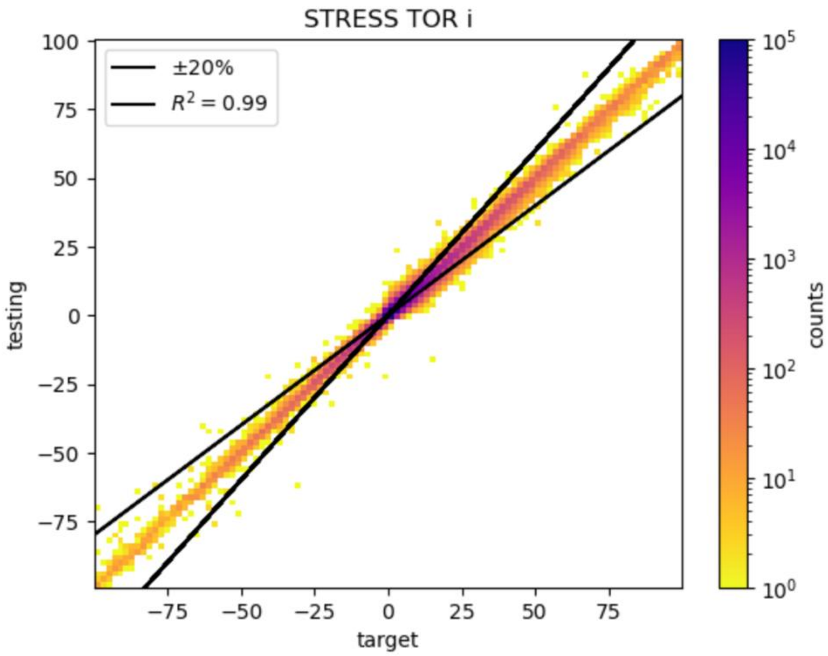

11 Components

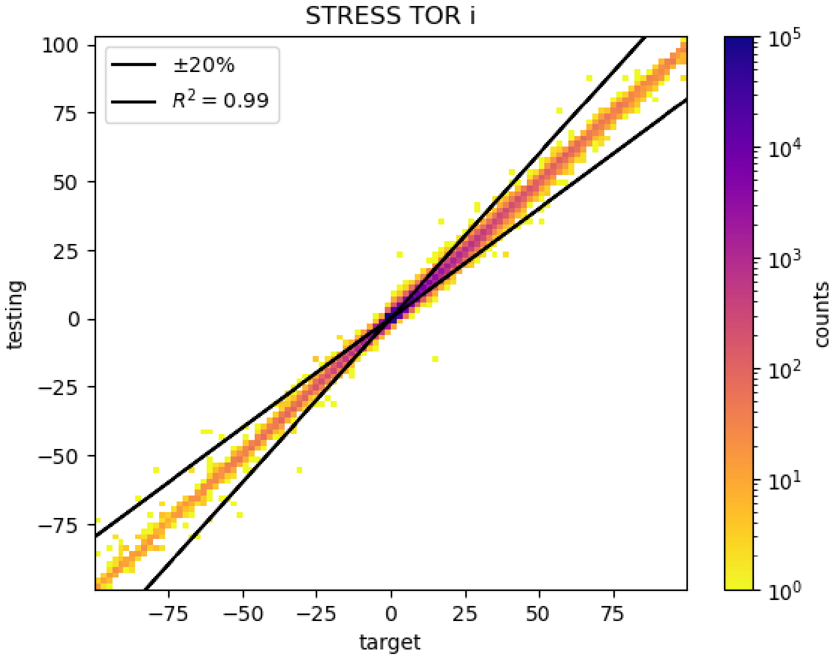

17 Components

OAK RIDGE National Laboratory

TGLF-NN-23D			
Variable	Definition	Database	Output
r/a	Normalized minor radius	RMIN_LOC	OUT_tur_ENERGY_FLUX_1
R/a	Normalized major radius	RMAJ_LOC	OUT_tur_ENERGY_FLUX_i
κ	Elongation	KAPPA_LOC	OUT_tur_PARTICLE_FLUX_1
$r\frac{\partial\kappa}{\partial r}$	Elongation shear	S_KAPPA_LOC	OUT_tur_STRESS_TOR_i
δ	Triangularity	DELTA_LOC	OUT_tur_PARTICLE_FLUX_2
$\frac{\partial R}{\partial r}$	Shafranov shift	DRMAJDX_LOC	OUT_tur_PARTICLE_FLUX_3
q	Safety factor	Q_LOC	
$\frac{q^2a^2}{r^2}\frac{\partial q}{\partial r}$	Safety factor shear	Q_PRIME_LOC	
β_e	Kinetic to magnetic pressure ratio	BETAE	
ν_{ie}/ac_s	Collision frequency	XNUE	
T_i/T_e	Ion to electron temperature ratio	TAUS_2	
n_D/n_e	Deuterium to electron density ratio	AS2	
n_C/n_e	Carbon to electron density ratio	AS3	

Z_{eff}	Effective ion charge	ZEFF	
a/L_{Te}	Electron temperature scale length	RLTS_1	
a/L_{Ti}	Ion temperature scale length	RLTS_2	
a/L_{ne}	Electron density scale length	RLNS_1	
a/L_{nD}	Deuterium density scale length	RLNS_2	
a/L_{nC}	Carbon density scale length	RLNS_3	
$\frac{qa^2}{rB_{unit}^2}\frac{\partial p}{\partial r}$	Total pressure gradient	P_PRIME_LOC	
$sign(I_p)R\omega_{tor}\frac{a}{c_s}$	Parallel velocity	VPAR_1	
$-sign(I_p)R\frac{\partial\omega_{tor}}{\partial r}\frac{a}{c_s}$	Parallel velocity gradient	VPAR_SHEAR_1	
$-sign(I_p)\frac{r}{q}\frac{\partial\frac{V_E\times B}{R}}{\partial r}\frac{a}{c_s}$	E x B velocity shear	VEXB_SHEAR	
λ_D	Debye length/gyroradius	DEBEYE	